POLYGENIC DETERMINANTS OF H5N1 ADAPTATION TO BOVINE CELLS

Matthew L Turnbull[1]*, Mohammad Khalid Zakaria1*, Nicole S Upfold1*, Siddharth Bakshi[1], Udeet Ranjan Das[1], Callum Magill[1], Laura Mojsiejczuk[1], Vanessa Herder[1,2], Kieran Dee[1], Nancy Liu[1], Monika Folwarczna[1], Georgios Ilia[1], Wilhelm Furnon[1], Verena Schultz[1], Hanting Chen[1], Ryan Devlin[3], Jack McCowan[3], Alex L Young[3], Wai-Wai Po[1], Katherine Smollett[1], Muhammad Ahsan Yaseen[4,5], Ana da Silva Filipe[1], Munir Iqbal[6], Ed Roberts[3], Joseph Hughes[1], Dirk Werling[7], Pablo R. Murcia[1**], Massimo Palmarini[1**]

[1]MRC-University of Glasgow Centre for Virus Research, Glasgow, UK

[2]CVR CRUSH, MRC-University of Glasgow Centre for Virus Research, Glasgow, UK

[3]CRUK Scotland Institute, Glasgow, UK

[4]Faculty of Veterinary Medicine, University of Teramo, Loc. Piano D'Accio, Teramo 64100, Italy

[5]Istituto Zooprofilattico Sperimentale dell' Abruzzo e Molise "G. Caporale", Teramo, Italy

[6]The Pirbright Institute, Woking, UK

[7]Centre for Vaccinology and Regenerative Medicine, Royal Veterinary College, London, UK

*These authors contributed equally to this work;

**Co-corresponding authors

ABSTRACT (200 words limit)

H5N1 avian influenza virus (lineage 2.3.4.4b, B3.13 genotype) has caused, unexpectedly, a large outbreak in dairy cattle in North America. It is critical to ascertain how this virus has specifically adapted to bovine cells and the molecular determinants of this process. Here, we focused on the contribution of the viral “internal” genomic segments of H5N1 B3.13 to bovine cells adaptation. We generated 45 reassortant viruses harbouring the haemagglutinin and neuraminidase from A/Puerto Rico/8/1934 and internal gene constellations from several influenza A viruses (IAV) or carrying segment swaps between distinct H5N1 strains. The recombinant B3.13 viruses displayed faster replication kinetics in bovine cells compared to other IAV. Importantly, multiple genomic segments of B3.13 viruses contribute to their faster replicative fitness. Further, recombinants with the B3.13 internal genes were less susceptible than ancestral 2.3.4.4b strain to the bovine IFN response. However, bovine (and human) MX1, a key restriction factor for avian IAV, restricted both ancestral 2.3.4.4b and B3.13 recombinant viruses. Interestingly, the latter escape restriction from human BTN3A3. Finally, recombinant B3.13 was virulent in mice unlike the ancestor 2.3.4.4b recombinant virus. Our results highlight the polygenic nature of influenza host range as multiple internal genes of B3.13 contribute to bovine adaptation.

INTRODUCTION

Influenza A viruses (IAVs) represent a major threat to human and animal health. These viruses have caused four human influenza pandemics and regular seasonal epidemics since 1918, in addition to panzootics, epizootics and outbreaks in wildlife and domestic animals[1-4]. IAV belong to the *Orthomyxoviridae*, possess eight single-stranded negative sense RNA genome segments, and are classified in subtypes based on their two surface glycoproteins: the haemagglutinin (HA; 19 subtypes) and neuraminidase (NA; 11 subtypes)[5].

Wild aquatic birds are the main reservoirs of IAV and harbour most of the known virus subtypes. Wild birds are a continuous source of infection for domestic birds, such as chickens and turkeys, which also harbour a variety of IAV subtypes. Humans, pigs, and horses instead are hosts to a limited number of IAV subtypes, which circulate in an endemic cycle within each species (e.g. H1N1 and H3N2 in humans).

Certain avian IAV subtypes including H5Nx, H7N9, H9N2, H10N8 and others, occasionally spill over into other mammalian species including humans. These spillover events almost never lead to documented mammal-to-mammal transmission chains, but they nevertheless represent a potential pandemic risk. Indeed, each of the four influenza human pandemics that have occurred since the 1918 H1N1 great influenza pandemic were caused by viruses carrying at least some genomic segments from avian influenza viruses (AIV)[6-10].

Within this context, highly pathogenic H5N1 is of particular concern as it is the cause of major devastating outbreaks in domestic chickens, and it has spilled over repeatedly in humans and other mammals[11]. Since 2021, H5Nx clade 2.3.4.4b has spread worldwide at unprecedented levels[12,13], and spilled into a variety of mammalian species such as skunks, raccoons, cats, bears, foxes[14-17] and aquatic mammals such as harbour seals and sea lions[18-21].

Unexpectedly, in March 2024, a reassortant between a European strain of H5N1 clade 2.3.4.4b and North American low pathogenic AIVs (classified as the B3.13 lineage) caused an outbreak of influenza in dairy cattle in the US[22]. Affected cows showed clinical signs such as fever, depression, drop in milk production and mastitis, but only rarely signs of mild respiratory

infections. Indeed, high levels of infectious virus could be detected consistently in the milk of infected animals[22]. The B3.13 lineage arose after a European-origin 2.3.4.4b entered North America in 2021[23,24], and subsequently acquired the PB2, PB1, NP and NS segments via sequential genetic reassortment events with low pathogenic avian influenza virus (LPAI) strains[24,25]. Phylogenetic analysis supports the notion that a single introduction event from wild birds into cattle occurred in late 2023 or early 2024 and this has subsequently spread to dairy farms across numerous states in USA[26]

Until this outbreak, cows had not been regarded as natural hosts of IAVs despite previous studies detecting anti-IAV antibodies in cattle sera, and experimental inoculations showing that cows are susceptible to both human and avian IAVs[27] (reviewed in [28]). Since its initial detection, H5N1 B3.13 has spread to 14 US states affecting over 400 dairy herds (as of November 2024)[29] . This virus has also spilled over to humans (25 confirmed human cases from contact with dairy cattle as of 9th November 2024[29]), in addition to cats and other small mammals in the vicinity of affected farms. Furthermore, a 2.3.4.4b virus but of a different genotype (B3.6) caused a limited outbreak in goats[30].

There are several known barriers to AIV adaptation in mammalian cells (reviewed in[31]). As obligate intracellular pathogens, viruses must use the cellular machinery to replicate their genome, synthesise viral proteins, and assemble into particles that in turn will be released to infect other cells either in the same or a different individual. In addition, viruses must overcome the host antiviral defences that include both innate (e.g. IFN, natural killer cells, macrophages, etc) and adaptive (e.g. cytotoxic T cells and antibody-producing B cells) immune responses. Successful virus replication thus requires a myriad of interactions between virus and host proteins and as a result, molecular incompatibilities and/or host antiviral mechanisms can act as effective host barriers.

The virus glycoproteins, and HA in particular, are key determinants of IAV host tropism. Avian HA favours binding to α2,3-linked sialic acid, which are abundant in the gastroenteric tract of birds, while the upper respiratory tract of humans and other mammals express mainly α2,6-linked sialic acid[32-36]. In addition, activation of HA of avian viruses after virus entry occurs at

higher pH levels compared to mammalian viruses. This property can lead to premature activation of avian-adapted HA extracellularly in the acidic mammalian respiratory tract (reviewed in [37]). The length of the NA glycoprotein stalk has also been associated with species-tropism[38].

However, important molecular determinants of virus host range include also viral proteins encoded by “internal” genomic segments (i.e. those encoding PB2, PB1, PA, NP, M, and NS). For example, the virus polymerase complex of avian viruses utilise less efficiently mammalian ANP32 proteins, which are essential cofactors for IAV replication[39-44] and the nuclear import machinery[45]. The nucleoprotein (NP) of avian viruses is the target of interferon stimulated genes MXA/ MX1 and BTN3A3, while human-adapted IAVs can escape these restriction factors[46-51]. The non-structural protein 1 (NS1) is a multifunctional protein, that counteracts the IFN response and is also associated with host-range[46,52,53].

Given the zoonotic nature of H5N1 IAVs, the size of the global cattle population (>1 billion[54]) and the high rate of contact between people and cattle (and cattle-derived products), it is essential to identify the viral determinants that facilitate bovine adaptation of H5N1. As determinants of host range are polygenic, reverse genetics approaches combined with quantitative assays are well suited to assess the contribution of individual genes to key fitness traits associated with host adaptation. These approaches constitute a biosafe, high throughput platform to develop predicting capabilities and to inform genomic surveillance systems about zoonotic risks.

Here, we sought to identify the virus genetic determinants that enabled H5N1 AIV to adapt to cows. Several other studies have concentrated on the H5N1 2.3.4.4b glycoproteins and their receptor preference[55-60]. Here, we concentrated specifically on the internal genes of European strains of 2.3.4.4b and the North American strains isolated from cows, humans and goats, in addition to other mammalian viruses used for comparative purposes. We assessed a set of 45 reassortants carrying identical glycoproteins in a variety of *in vitro*, *ex-vivo* and *in vivo* assays to assess replication kinetics, polymerase activity, sensitivity to type-I IFN and restriction factors, and virulence in animal models.

RESULTS

Reassortants generated in this study. To investigate the molecular determinants of H5N1 B3.13 adaptation to the bovine host, we derived by reverse genetics a set of 6:2 reassortants carrying the glycoproteins (HA and NA) of the laboratory-adapted H1N1 A/Puerto Rico/8/34 (PR8) strain, and the internal genomic segments (i.e. those expressing PB2, PB1, PA, NP, M, and NS) of phylogenetically distinct IAVs (Fig 1).

Using reassortant viruses carrying identical glycoproteins allowed us to focus specifically on the potential role of the other viral proteins in adaptation to bovine cells in biosafe conditions. Each reassortant used in this study is termed using the prefix "r" followed by an abbreviated name of the strain in question (Table 1). Reassortants from H5N1 include viruses involved in the North American outbreak. r-Cow(H5N1) possesses the internal genes from one of the early bovine influenza sequences (sample acquired from a dairy cow on 20th March 2024 in Texas). r-Texas/37(H5N1) is a similar, but distinct, B3.13 strain that infected a dairy farm worker and likely derives from a common ancestor of the lineage that has spread in cattle[26]. r-goat(H5N1) possesses the internal genes from the 2.3.4.4b virus isolated in goats (B3.6 genotype)[30]. We also generated a panel of reassortants with the internal genes of several other IAV from different hosts. These include the following: European-origin early H5N1 2.3.4.4.b avian viruses ancestral to the B3.13 strains [r-AIV07(H5N1), r-AIV09(H5N1), and r-AIV48(H5N1)], the pandemic human 2009 virus [r-pdm09(H1N1)], avian H7N9 isolated in a spillover event in humans [r-Anhui/13(H7N9)], a swine-origin virus isolated from a spillover event in humans [r-Eng/23(H1N2v)], equine IAV [r-Equine(H3N8)], and canine IAV [r-Canine(H3N8)] (Table 1). We also generated 4:4 reassortants containing HA, NA, M and NS from PR8 and only the polymerase complex (PB2, PB1, PA and NP) from the viruses of interest. We derived these reassortants specifically to assess the activity of the polymerase complex and sensitivity to the restriction factor MX1[51] (Table 2); these include some of the viruses indicated above [r-Cow(H5N1), r-Texas/37(H5N1), r-Goat(H5N1), r-AIV07(H5N1), r-AIV09(H5N1), r-AIV48(H5N1), r-Eng/23(H1N2v), r-Anhui/13(H7N9)], and others of avian [r-Arg(H4N2), r-

Chn/23(H3N8), r-Mld/99(H1N1), r-Nld(H7N7), r-Chn/13(H10N8)], or swine [r-Iowa/11(H2N2v), r-Ohio/16(H3N2v)] origin. Of note, with the exceptions of r-Arg(H4N2) and r-Mld/99(H1N1), all the other sequences of the segments used in these latter reverse genetic constructs were derived from viruses involved in spillover events in humans. It should, however, be noted that the virus from which the reverse genetics constructs were derived for Mld/99(H1N1) had been previously passaged in pig cells[61]. All reassortants were rescued in HEK-293T cells and propagated in MDCK to prepare viral stocks as described in Methods. Wild type PR8 was used as control.

North American 2.3.4.4b reassortants display the fastest replication kinetics in bovine cells. We first assessed the replication kinetics of the reassortant viruses in MDCK cells, as this canine cell line is considered to be permissive to most IAVs. Indeed, most reassortants replicated efficiently (Fig 2a), apart from r-Anhui/13(H7N9) and r-Eng/23(H1N2v) which displayed slower replication kinetics at 24 hours post-infection (hpi). Next, to determine the replication fitness of the reassortant viruses in a bovine cellular context, we assessed their replication kinetics in bronchial explants, primary cells, and cell lines derived from cattle. All reassortants displayed minimal or no replication in bovine tracheal explants, mammary-tissue derived epithelial cells[62] and immortalised bovine endothelial cells[63] (Fig S1). However, both an IFN-competent cell line that we derived from bovine skin fibroblasts[63], and primary nasal fibroblasts, were permissive to infection by all reassortants (Fig 2b-c; Fig S2). These cells enabled us to observe differences in replication kinetics between the reassortant viruses. r-Tx/37(H5N1), r-Cow(H5N1) and r-goat(H5N1) displayed faster replication kinetics, reaching higher virus titres than their European-origin 2.3.4.4b counterparts [r-AIV07(H5N1), r-AIV09(H5N1), and r-AIV48(H5N1)], and diverse mammalian-origin IAVs at 24 hpi. All viruses reached similar titres by 48-hpi (Fig 2b). A similar trend was observed in bovine primary nasal fibroblasts (Fig. 2b-c), regardless of whether subsequent virus production in the supernatant was measured in infectious units or by viral RNA (Fig S2). Overall, these data suggest that the internal genomic segments of B3.13 IAVs provide a kinetic advantage *in vitro* relative to the 2.3.4.4b ancestral viruses circulating in avian hosts in Europe, and to IAVs from other

mammalian hosts, suggesting that the B3.13 internal gene constellation provides a fitness advantage in bovine cells over the ancestral viruses. The closely-related, but distinct, goat-derived 2.3.4.4b virus also displayed virus replication kinetics similar to the B3.13 reassortant viruses, suggesting that more than one constellation of internal genomic segments increases replication fitness.

Polymerase activity of B3.13, related avian H5N1 and other IAV in mammalian cells. The polymerase complex (PB1, PB2, PA and NP) is one of the critical determinants of IAV host tropism. As the viruses we assessed above exhibited different replication kinetics, we next performed standard minireplicon assays to assess the contribution of the polymerase to the phenotype observed. We tested the polymerase complexes of the H5N1 B3.13 viruses, the North American H5N1 isolated from goats, the ancestral avian European H5N1 and a variety of other control viruses for comparative purposes. In addition to the polymerases from viruses in figure 2, we used those from the Hong Kong 1968 human pandemic virus, swine viruses isolated from spillover events in humans, avian viruses also isolated from spillover events in humans and avian viruses never described to be transmitted into humans. This extensive set of polymerases allowed us to obtain a comprehensive and comparative overview of their activity in mammalian cells.

From the results of our assays (Fig 3a) we could arbitrarily divide the polymerases into the following 4 groups based of the levels of their activity: (i) very high, (ii) high, (ii) medium and (iv) low (Fig 3a). The polymerases with the highest activity were those of the H3N2 Hong Kong 1968 pandemic virus, the H5N1 B3.13 Tx/37, and those of the zoonotic avian viruses H7N9, H7N7, and H10N8. With the exception of PR8, these polymerases were the only ones among those tested that contained the well-known PB2 E627K “mammalian” adaptive mutation (Fig. 3a).

The group with high polymerase activity included PR8, the H1N1 2009 pandemic virus, and three swine viruses isolated from spillover events in humans (H1N2v and H3N2v). This group of polymerases instead uniquely possess the mammalian adaptive mutation PB2 T271A. Only PR8 contained both PB2 E627K and T271A. Polymerases of the ancestral 2.3.4.4b

H5N1(AIV48) and the cow/H5N1 displayed medium polymerase activity. Interestingly, the sequence of PB2 derived from cow H5N1 did not possess any major known PB2 adaptive mutations, with the exception of M631L which has been reported to boost polymerase activity and has been shown to contribute to activity of a B3.13 polymerase in human cells[64,65]. The viruses with the lowest polymerase activities among those tested were those from the avian viruses H1N1 (1999, Netherlands), 2.3.4.4b H5N1 AIV09 and AIV07, H4N2 (Argentina, 2011), and H3N8 (China, 2023). Interestingly, the 2.3.4.4b H5N1 isolated from goats also displayed relatively low polymerase activity (approximately 5-fold compared to the cow H5N1 and 100-fold against Tx/37).

Given the differences in polymerase activity noted between the polymerases of 2.3.4.4b (ancestral avian) and the North American B3.13 viruses, we assessed which genomic segment(s) of the latter conferred a higher polymerase activity in mammalian cells. We therefore compared the activity of single subunit swaps between the polymerase complex of (i) cow B3.13, (ii) human Tx/37 and the ancestral 2.3.4.4b AIV07 (Fig 3b-c). Individual substitution of cow H5N1 or Tx/37 H5N1 polymerase subunits with PB1, PA or NP subunits from AIV07 did not significantly reduce r-Cow or r-Tx/37 polymerase activity. However, substitution with AIV07 PB2 decreased both r-Cow and r-Tx/37 polymerase activity, although only significantly for r-Tx/37. These data were confirmed by the reciprocal swaps in the AIV07 polymerase complex (Fig. 3c). The AIV07 polymerase reached similar levels of activity to Tx/37 when the PB2 subunit of the latter was introduced, while neither PA nor NP derived from Tx/37 made a difference to AIV07 polymerase activity. Introduction of TX/37 PB1 increased AIV07 polymerase activity by approximately 10-fold, although this was not statistically significant. Similar results were obtained with the swap constructs between the polymerase subunits of cow H5N1 and AIV07 polymerases (Fig. 3c).

The combination of the B3.13 polymerase genes confers a replication advantage in bovine cells. The data obtained above suggest that PB2 is a key determinant of 2.3.4.4b mammalian adaptation. The replicon assays, however, measure polymerase activity in transfected 293T cells but do not assess the whole viral replication cycle. In addition, as 293T

are human cells they may fail to capture bovine-specific adaptive features. We therefore carried out virus replication assays in bovine fibroblasts using PR8-based reassortant viruses. In these experiments, we introduced the four internal genomic segments acquired by B3.13 viruses from a low pathogenic avian influenza virus from North America[24,25]. Specifically, PB2, PB1, NP and NS were swapped between r-Tx/37(H5N1) or r-Cow(H5N1) and the ancestral r-AIV07(H5N1) (Fig 4a-b). We measured virus titres at 24hpi where the fastest replication kinetics of the B3.13 reassortants were most evident (Fig 2). Individually replacing the PB2, PB1, NP or NS segments in either of the B3.13 viruses [r-Cow(H5N1) or r-Tx/37(H5N1)] with those of the AIV07 ancestor did not reduce virus titres to the level of r-AIV07(H5N1) in bovine skin fibroblasts (Fig 4a). Of note, the r-Cow(H5N1) reassortant containing the AIV07 PB2, reached significantly lower titres than complete r-Cow(H5N1). However, the largest reduction in virus replication was observed when we simultaneously inserted PB2, PB1, NP and NS of r-AIV07(H5N1) into r-Cow(H5N1). This reassortant, referred to as r-Cow:AIV07 QUAD, displayed a 6:2 combination with only the PA and M segments from a B3.13 origin. Similar results were obtained with reassortants between r-Tx/37(H5N1) and AIV07(H5N1) (Fig 4b). Both r-Cow:AIV07 QUAD and r-Tx/37:AIV07 QUAD displayed the largest reduction in virus titres compared to the complete B3.13 reassortants, although neither reached the levels of the r-AIV07(H5N1) control. When the B3.13 segments were reciprocally introduced into the ancestral r-AIV07(H5N1), only the combination of all four segments could rescue viral replication to levels approaching the r-Cow and r-Tx/37 controls (Fig 4b). Therefore, in the context of a replicating virus, the increased polymerase activity in human cells provided by B3.13 PB2 is not sufficient for the increased kinetics in bovine cells, if not in combination with homologous PB1, NP and NS.

To further explore the role of the polymerase subunits in virus replication, we rescued 4:4 recombinant viruses in which the polymerases complexes (PB2, PB1, PA and NP) were paired with the HA, NA, M and NS from PR8, and compared these to the aforementioned 6:2 viruses. When bovine cells were infected with 4:4 or 6:2 viruses in parallel, it was firstly evident that each virus replicates more efficiently when its cognate M and NS segments were present (Fig

4c-d). Secondly, the 4:4 viruses of B3.13 origin replicated more efficiently than counterpart ancestral avian-derived H5N1 4:4 viruses, suggesting that the B3.13 polymerase complex confers an advantage in the absence of the M and NS segments. Interestingly, the r-Texas/37(H5N1) 4:4 virus had faster replication kinetics than the r-cow(H5N1) 4:4 equivalent, suggesting that the human-derived Texas/37 polymerase complex is fitter in bovine cells than the cow-derived counterpart, which is consistent with polymerase activity data described in human cells (Fig 3a). However, in the form of 6:2 viruses there was no distinction between these two strains when infected in parallel, suggesting that the presence of the cognate M and NS segments can overcome differences in replication efficiency. Furthermore, at 24 hpi, the differences in titres between B3.13 recombinant viruses and 2.3.4.4b avian-derived viruses appeared starker as 6:2 viruses than as 4:4 viruses, potentially further pointing to roles for M and NS and/or epistatic interactions.

Decreased sensitivity of B3.13 viruses to the bovine type-I IFN response. The host type-I IFN response is another important barrier to virus cross-species transmission. Hence, we compared the susceptibility of the B3.13 reassortants, r-Cow(H5N1) and rTx/37(H5N1), and of the ancestral avian-derived r-AIV07(H5N1) to the bovine type-I IFN response. First, we confirmed that stimulation of bovine fibroblasts with universal type-I IFN resulted in the activation of markers of a type-I IFN response. As expected, western blot analysis of IFN-treated bovine fibroblasts showed a dose-dependent upregulation of phosphorylated Stat1 (pSTAT1), and of the ISGs MX1 and RSAD2 (Fig. 5a).

Next, we compared the susceptibility of r-Cow(H5N1), r-Tx/37(H5N1) and r-AIV07(H5N1) to IFN by assessing their replication in pre-stimulated or mock-treated bovine fibroblasts. All viruses showed sensitivity to IFN in a dose-dependent manner (Fig 5b). However, r-AIV07(H5N1) displayed a greater susceptibility to the bovine IFN response than the B3.13 viruses, or PR8 used as control. For example, at 24 hpi, pre-stimulation of bovine fibroblasts with 40U/ml of IFN was sufficient to completely inhibit replication of AIV07 below the detection limit, while both r-Cow(H5N1) and r-Tx/37(H5N1) reached titres around 10^4/ml in the same

conditions. At 48 hpi, 1.6 U/ml of IFN had no effect on r-Cow(H5N1) titres, but reduced r-AIV07(H5N1) titres 150-fold on average (Fig. 5b, right).

The key effectors of the type-I IFN response are ISGs, some of which can directly hamper virus replication, and therefore transmission and/or pathogenicity[66-68]. One of the important ISGs in the context of IAV cross-species transmission is MX1 (dynamin-like GTPase myxovirus-resistance Gene 1), which targets vRNPs in a strain-dependent manner[46,48-51] and restrict avian-origin viruses that do not possess escape mutations. Fig. 5a indicates that this restriction factor is upregulated in bovine cells, upon stimulation with universal type I IFN. We next asked whether MX1 expression could be detected in the udders of dairy cows following infection, as this appears to be a major site of productive infection in cows[24,55,69]. We cultured and infected precision-cut udder slices from dairy cows with r-Tx/37(H5N1), r-Cow(H5N1), r-AIV07(H5N1) and r-AIV048(H5N1). After 72 hours we fixed and immunostained tissue sections for viral NP and MX1. Infection was very inefficient and only two slices, both infected with r-Tx/37(H5N1), showed abundant NP staining in the duct epithelium. Although this experiment was inconclusive with respect to infection with our virus panel, Mx1 expression was clearly detected in the infected cells of the duct epithelium (Fig 5c-d).

Bovine Mx1 inhibits B3.13-derived reassortants. Next, we aimed to determine whether MX1 restricts bovine influenza virus. The key IAV determinant of MX1 activity is the viral NP. As our 6:2 reassortants carry the NP of bovine influenza virus (and viruses of interest) they are a suitable system to evaluate the susceptibility of different IAVs to MX1 restriction. To this end, we constitutively expressed human, bovine or rat MX1 in bovine fibroblasts and human A549 cells (Fig 6a). In human A549 cells, both bovine and human MX1 displayed antiviral activity against a r-Tx/37(H5N1) reporter virus in a single-cycle infection relative to a chicken MX1 control gene (lacking antiviral activity[70-72]) by approximately 3-fold, while PR8 was affected by less than two-fold relative to the chicken MX1 control cells (Fig 6b). Neither MX1 proteins displayed the strength of antiviral activity exhibited by the rat MX1 control, a known potent antiviral gene against IAV[73]. In a low MOI, multicycle assay, both human and bovine Mx1 exhibited antiviral activity against the B3.13 reassortants, although restriction of these

viruses was not as pronounced as against avians r-AIV07(H5N1) or r-Mld/99(H1N1) (Fig 5c). Furthermore, both human and bovine MX1 proteins retained their antiviral properties against a wide array of both 6:2 and 4:4 reassortants (Table 2) when overexpressed in bovine skin fibroblasts (Fig 6d-e) suggesting that these proteins can function in both the human and bovine cell contexts. All the reassortants based on 2.3.4.4b H5N1 were restricted by both bovine and human MX1. As expected, all the reassortants based on avian viruses, with the notable exception of H10N8, were restricted by bovine MX1. On the other hand, PR8 and reassortants derived from zoonotic events of swine viruses [r-Eng/23(H1N2v), r-Iowa/11(H3N2v) and r-Ohio/16(H3N2v)] were not significantly inhibited by bovine MX1 (Fig 6e). Hence, these results show that bovine MX1 is an effective antiviral gene.

Another ISG that specifically restricts most avian viruses and also acts on the viral NP is BTN3A3[46]. MX1[47-51] is conserved in most vertebrates, including cattle, while BTN3A3 originated specifically during the evolution of old world mokeys[46], and therefore cannot play a role in H5N1 adaptation to cow cells. However, this restriction factor is one of the important human host genetic barriers to avian IAV zoonotic transmission. Hence, we assessed the replication of a selection of our reassortant viruses, including PR8 and r-Mld/99(H1N1) as controls, in MDCK overexpressing BTN3A3 or in the parental cells (Fig 6f-g). As expected, PR8 replicated equally well in parental and BTN3A3 expressing cells, while r-Mld/99(H1N1) replication was substantially inhibited in the latter. Among the reassortants tested, only r-Goat(H5N1) was restricted by BTN3A3, while all the other 6:2-based 2.3.4.4b or B3.13 viruses evaded this important restriction factor (Fig 6g). Hence, many 2.3.4.4b viruses already possess NP mutations that evade BTN3A3 restriction.

r-cow(H5N1) is more virulent than r-AIV07(H5N1) in mice. Experimental infection in mice is often used as a proxy to test IAV virulence (reviewed in [74]). Therefore, we next infected BALB/c mice with 100 PFU of either r-Cow(H5N1), r-AIV07(H5N1) or PR8 as control. PR8, a mouse-adapted laboratory strain, caused severe weight loss in infected animals, while the weight of mice infected with r-AIV07(H5N1) was essentially unaffected. Mice infected with r-Cow(H5N1) displayed an intermediate phenotype showing weight loss but not as severe as

those infected with PR8 (Fig 7a). Both quantification of NP in the lungs of infected mice euthanised at 3 days post-infection (dpi) and T-cell infiltrates (CD3) in mice euthanised at 8 dpi displayed similar trends, with higher values in mice infected with PR8, followed by those infected with r-Cow(H5N1) and then r-AIV07(H5N1), although differences were not statistically significant due to variability within groups (Fig 7b-d). No significant differences in the levels of B cells (PAX5) were observed between the groups at 8 dpi (figure 7e). As highly pathogenic H5N1 can induce a systemic infection, we also assessed the presence of NP in the brains of experimentally infected mice to determine virus spread in organs other than the lungs. We could not detected viral NP by immunohistochemistry in any brain of the infected animals (not shown). Lack of systemic infection by r-Cow(H5N1) was to be expected as HPAI HA is a key determinant of systemic infection[75,76].

DISCUSSION

While a multitude of direct IAV avian-to-mammal interspecies infections have been reported over the years, only a few avian viruses have established as endemic mammalian lineages. Prior to the panzootic spread of clade 2.3.4.4b H5N1 from 2021, viruses considered to emerge directly from birds included the Eurasian swine H1N1 lineage[77], the H7N7 and two H3N8 lineages[78 79,80] of equine influenza viruses, and the H3N2 canine influenza lineage[81]. Relevant to our work, all human pandemic viruses carried at least one avian-origin internal genomic segment[9,82 6-10].

The number of spillover events of HPAI H5N1 in mammals appear to be ever expanding[11] and is associated with a global increase in prevalence of clade 2.3.4.4b. In 2022, two separate introductions of H5N1 2.3.4.4b resulted in mammal-to-mammal transmission, as documented by outbreaks in mink in Spain[83] and marine mammals in South America[18,20,21,84]. These viral incursions highlighted the propensity of H5N1 2.3.4.4b to adapt to phylogenetically distant mammalian hosts. This is reinforced by the ongoing epizootic of H5N1 HPAI in dairy cattle, which provides the clearest example of a direct transfer of an entire avian IAV into a new mammalian host. The large numbers of farmed cattle, the close contact of dairy cows with

humans, and the high titres of virus in milk and unpasteurized dairy produce make the current situation particularly concerning, especially as reports of zoonotic infections in dairy farm workers keep increasing[29].

In this study, we assessed the role of the internal genomic segments (those encoding PB2, PB1, PA, NP, M and NS) on the adaptation of B3.13 viruses to bovine cells. We focused on replication fitness and sensitivity to bovine type-I IFN and key restriction factors. In addition, we examined the contribution of the internal genomic segments of B3.13 viruses to virulence using an established animal model. We compared H5N1 B3.13 against a panel of diverse strains including European-origin ancestral avian H5N1, other avian viruses (some of them involved in documented zoonotic events) and viruses circulating in humans, pigs, dogs and horses. We tested in total 45 reassortant viruses including different combinations where we swapped genomic segments between distinct H5N1 strains.

Our results indicate that the constellation of internal genomic segments of the B3.13 genotype provides a replication advantage in bovine cells over other IAVs. Assays with reassortants between B3.13 viruses and an ancestral European 2.3.4.4b H5N1 strain revealed that the increased replication fitness in bovine cells resulted from the acquisition of multiple segments through sequential reassortment events involving European-origin H5N1 and American LPAI viruses[24,25]. Furthermore, we showed that the polymerase complex of B3.13 was sufficient to provide a substantial change in replication phenotype. The internal genes of a closely related, but distinct, B3.6 genotype virus (that caused a spillover in goats and carries a phylogenetically different PB2[30]), also replicated to similar levels as the B3.13 recombinant viruses in bovine cells, suggesting that multiple evolutionary pathways can achieve increased replication fitness in bovine cells. Of note, both the cow- and human-derived B3.13 strain have acquired separate mammalian-adapted mutations in their polymerases not seen in ancestral B3.13 strains. A/Texas/37 (H5N1) acquired the well-described mammalian-adaptation mutation PB2-E627K, a relatively frequent avian-to-mammalian mutation that enhances cooperation with human ANP32 proteins[39,85], which is absent in the PB2 of H5N1 detected in cattle. Bovine IAV instead acquired a separate set of mammalian adaptive mutations including PB2-M631L and PA-

K497R[65,86]. Importantly, a recent study reported that PB2 631L improves polymerase activity of a B3.13 H5N1 in human cells[87].

We observed differences between the polymerase activity as assessed by replicon assays in human cells, with virus replication assays in bovine cells using either 4:4 or 6:2 reassortant viruses. Using a panel of 18 IAV polymerases in replicon assays we showed that those carrying PB2 627K, including B3.13 H5N1 Tx/37, displayed the highest polymerase activity in human cells, significantly higher than the bovine- and goat-derived H5N1 polymerases. Our data with full virus replication assays in bovine cells, using 4:4 reassortants with the polymerase complex of the virus of interest, supported some of the differences noted above [Tx/37(H5N1) > cow(H5N1) > AIV07(H5N1)]. However, some of the reassortant viruses, such as r-goat(H5N1) and the r-Texas/37 reassortants with the AIV07 PB2, do not have PB2-627K, PB2-631L nor PA-497R mutations and yet exhibit robust replication in bovine cells, highlighting that some of the well-known adaptive mutations in IAV polymerase are not strictly required as other residues and/or epistatic interactions can permit efficient replication in bovine cells. This notion is reinforced by our comparison of 4:4 with 6:2 reassortants, which also suggests a synergistic role for segments M and NS in B3.13 adaptation to bovine cells.

Importantly, the B3.13 reassortant viruses were less sensitive to the bovine type-I IFN response compared to an ancestral 2.3.4.4b virus. However, we found H5N1 B3.13 to be restricted by bovine (and human) MX1, one of the key restriction factors blocking avian IAV replication[47-51]. We also show that bovine MX1 is expressed in infected bovine cells, including mammary tissue, the major site of bovine B3.13 H5N1 replication in cows[24,55,69]. Hence, differences in IFN-sensitivity between B3.13 and ancestral avian viruses may be due to other ISGs or to differential kinetics of virus replication inducing either a faster inhibition of the cell-autonomous IFN response or generalised cell transcription/ translation.

Although we showed that virus polymerase activity in human cells does not necessarily correlate with replication kinetics in bovine cells, we also showed that the r-H5N1-Cow virus caused more severe infection than the ancestral r-H5N1-AIV07 virus in a mouse model, suggesting that the former has already acquired mutations enhancing its virulence in a

mammalian host. Hence, it is feasible to think that the current level of adaptation of B3.13 to mammals, may give the virus the opportunity to acquire mutations that bring it closer to crossing the species barrier into humans[88]. Our data also suggest that B3.13 already can escape BTN3A3 restriction[46], another key human genetic barrier to avian IAV. With regards to MX1, we showed that the bovine and human orthologs can restrict H5N1 B3.13 replication, although often not at the same levels of some other avian viruses. Hence, bovine MX1 may provide a selective pressure on cow H5N1 to select mutants that could increasingly escape the human and bovine MX1 orthologues. Future research on this area is crucial to risk assess this virus' potential to emerge in humans.

We acknowledge some limitations of this study. We specifically focused on the internal genomic segments of B3.13 and therefore have used recombinant viruses harbouring the HA and NA of a laboratory-adapted H1N1 strain (PR8). Consequently, cells that may not be permissive to a recombinant virus harbouring the glycoproteins of PR8 may be susceptible to infection by an authentic B3.13 H5N1 virus and *vice versa*. For this reason, we used primary immortalised bovine skin fibroblasts and primary nasal fibroblasts as cell model systems. These cells allowed us to explore species-specific virus-host interactions within a bovine intracellular context as they express required cellular co-factors, are IFN competent and express known IAV-restriction factors (e.g. MX1). Another potential limitation is the use of reassortants in general. While they are exceedingly useful tools to map molecular determinants of specific phenotypes, they could also in some cases possess defects due to incompatibilities between genome segments that have not co-evolved together.

Overall, our study characterised the internal genomic segments of B3.13 with great level of detail and compared them with a wide variety of other IAVs able to infect disparate hosts. We demonstrated that the internal genomic segments of B3.13 viruses circulating in cattle have enhanced replication capacity in bovine cells, raising concerns that the virus may be one step closer to causing outbreaks in humans.

METHODS

Phylogenetic analysis. Influenza A virus sequences were retrieved from the NCBI Entrez databases using the Influenza A virus taxonomic ID with an in-house Python tool to access the E-utilities API. This dataset was further enriched with sequences from GISAID matching the search term “Clade=2.3.4.4b” and consensus genomes available in Andersen Lab's public GitHub repository (https://github.com/andersen-lab/avian-influenza). All databases were last accessed on September 1st, 2024. Fasta sequences were sorted by genomic segment and redundancies between databases were removed based on strain name. The MMseqs2 software tool v15.6f452 was used to cluster the sequences based on a 0.95 identity threshold and select a representative sequence per cluster (--cluster-mode 2 --cov-mode 1 --min-seq-id 0.95)[89], resulting in the following number per genomic segment: PB2: 458, PB1: 406, PA: 405, NP: 221, MP: 112, NS: 222. Representative sequences per segment along with the sequences of the viruses of interest (detailed in Table 1) were aligned using MAFFT v7.453 using the default parameters[90]. Maximum likelihood trees were obtained with IQ-tree v2.1.2 under the best-fit model and plotted in RStudio using ggtree v3.12.0[91,92].

Generation of reassortant viruses harbouring PR8 HA and NA glycoproteins. pHW2000 reverse genetics plasmids used to rescue the A/California/04-061-MA/2009(H1N1) virus were a kind gift of Prof. Daniel Perez, the A/mallard/Netherlands/10-Cam/1999(H1N1) virus from Prof. Laurence Tiley, A/Puerto Rico/8/1934 (H1N1) virus from Prof. Ron Fouchier, and the A/canine/Illinois/11613/2015 (H3N2) from Prof. Luis Martinez-Sobrido. pHW2000 reverse genetics plasmids to rescue the A/England/2023 (H1N2v) and A/Texas/37/2024 (H5N1) viruses were synthesised and cloned by GeneArt Thermo Fisher. Each gene segment from A/equine/South Africa/4/2003(H3N8) was subcloned into pHW2000 following RT-PCR from RNA extracted from virus.

6:2 viruses with the HA and NA genes from PR8 (Table 1) were rescued by reverse genetics. HEK-293T cells were transfected with pHW2000 reverse genetics plasmids (250 ng of each plasmid in 6-well plate format) and the media changed to ‘virus growth medium’ (serum-free DMEM supplemented with 1 ug/mL TPCK-trypsin (Sigma) and 0.14% (w/v) BSA fraction V (Gibco)) at 16 h post-transfection. Supernatant was collected at 48h post-transfection and

used to inoculate cultures of MDCK cells maintained in virus growth medium until approximately 70-80% of cells displayed cytopathic effect. At this point the supernatant was clarified by centrifugation prior to storage at –80 °C in small volume aliquots. All infections were carried out with previously unthawed virus aliquots to avoid freeze-thaw changes to infectious titre. All viruses used have been sequenced to confirm identity.

Cells. Cells were maintained in DMEM (Gibco 31966021) supplemented with 9% (v/v) HI-FCS (Gibco), 100 U/mL Penicillin and 100 µg/mL Streptomycin (Gibco) (hereafter referred to as 'complete DMEM') at 37°C with 5% CO_2 unless otherwise stated. HEK-293T, MDCK and A549 cells have been described previously[46]. Primary-derived bovine skin fibroblasts have been described previously[93]. Nasal respiratory epithelium from the turbinates of the cow were collected from the abattoir in complete DMEM media containing 10% FCS, 100 U/mL Penicillin and 100 µg/mL Streptomycin (Gibco) and 2.5 µg/mL Amphotericin B as an antibacterial and antifungal agents respectively. Tissues were washed three times with PBS and incubated in 10 ml of complete DMEM media containing collagenase (2 mg/ml, collagenase from *Clostridium histolyticum*, Sigma) at 37°C for 2h. Subsequently, supernatant was strained with 70 µm strainer (Greiner) and subsequently centrifuged at 188 *x g* for 5 minutes. The cell pellet generated was washed three times in complete DMEM media to remove collagenase. Cells were finally cultured in complete DMEM and incubated at 37°C, 5% CO_2. Media was changed every day initially to remove non adherent cells until an adherent population of fibroblasts was achieved; cells were subsequently passaged using standard procedures. All infection experiments were carried out with early passages cells (before stationary phase was achieved) as described below.

Bovine Mammary Epithelial-UV (BME-UV) cells[62] were provided by Dr Paolo Accornero (Universita' di Torino). They were maintained in 50:50 Ham's F-12 Nutrient Mix (Life technologies 21765029) and DMEM GLUAMax (Life Technologies 31966021) supplemented with 10 ng/ml Epidermal Growth Factor, 5 µg/ml Insulin (Merck I2643), and 10% (v/v) fetal bovine serum.

For infections, cells were seeded in 12-well plates at $5x10^5$/well approximately 24 hours prior to infection. Confluent monolayers were infected with 10^3 genome copies equivalent of virus. Virus was adsorbed for 1h, removed and replaced with infection media - 50:50 Ham's F-12 Nutrient Mix and DMEM GLUAMax supplemented with 10 ng/ml Epidermal Growth Factor (Merck SRP3027) , 5 µg/ml Insulin (Merck I2643), 1 µg/ml TPCK-trypsin and 0.14% (v/v) BSA fraction V. Samples were taken at the indicated timepoints and replenished with the same volume of fresh media.

BTN3A3 overexpression cell lines have been described previously[46]. To overexpress MX1, the Mx1 genes of *Rattus norvegicus* (GenBank accession NM_173096.3), *Bos taurus* (GenBank accession NM_173940.2), *Homo sapiens* (GenBank accession NM_002462.5) and *Gallus gallus* (GenBank accession NM_204609.2) were synthesised by BioBasic and subcloned into the SCPRSY lentiviral vector. Cell were modified by lentiviral transduction using SCRPSY vectors using standard techniques as previously described[94].

Virus replication assays. Typically, cells were plated in 12-well plates the day prior to infection. Cells were washed with serum-free DMEM prior to infecting with 200 µL of virus diluted in serum-free DMEM to achieve desired MOI. After 1 h of incubation, the inoculum was removed and cells were overlaid with 1 mL of virus growth medium. Plaque assays to titrate infectious virus in the supernatant of infected cells were performed as described previously[46]

Quantification of viral RNA. Infected culture supernatants were homogenized in Trizol LS reagent (Thermo Fisher), and viral RNA was extracted using the Direct-zol-96 MagBead RNA kit (Zymo Research, R2102) automated on the KingFisher Flex System (Thermo Fisher) as per the manufacturers' instructions. To quantify negative-sense vRNA and avoid non-specific priming of positive-sense replication intermediates, quantification was carried out as a two-step RT-qPCR. Specifically, vRNAs were reverse transcribed using SuperScript IV (Thermo Fisher) and the Uni12 primer[95] in half-reactions containing 2.5 ul of extracted RNA. qPCR was performed using Fast SYBR Green Master Mix (Thermo Fisher), and HA fragment specific primers: IAV_HA_For 5′ AAACAGCAGTCTCCCTTTCCAG and IAV_HA_Rev: 5′

GTTCCTTAGTCCTGTAACCATCCTCA. Each reaction contained 4 ul of cDNA and was run using an ABI7500 Fast instrument, according to the manufacturer's recommendations, and results were analysed with the 7500 Software v2.3 (Applied Biosystems, Life Technologies). A 714 bp synthetic gBlock carrying a partial sequence of PR8 HA (Twist Bioscience, custom) was used to generate a standard curve. Viral load was extrapolated from the curve and viral genomes were expressed as number of HA gene copies per ml of supernatant.

Polymerase activity assays. Subconfluent monolayers of 293T cells (1.5 x 10^5 cells seeded in 24-well plates the day prior to transfection) were co-transfected with 10 ng each of pDUAL bi-directional plasmids encoding PB2, PB1, PA and transfection control plasmid (CMV-driven expression of Renilla luciferase) and 25 ng each of NP and a PolI-driven expression of cRNA-driven expression of luciferase reporter plasmids, in Gibco™ Opti-MEM™ Reduced Serum Medium, using Invitrogen™ Lipofectamine™ 2000 CD Transfection Reagent. Transfection lacking the NP plasmid served as negative control. 24 hours post-transfection, the transfection medium was removed, and cells were lysed by adding 100 µl of 1X-passive lysis buffer (Dual-Luciferase reporter assay system, Promega), and freeze-thawing. The lysates were transferred to white-walled 96-well plates (Greiner) and luminescence was measured from 20 µL of lysate by using 30 µL of either luciferase assay reagent II or STOP & Glo reagent (Dual-Luciferase reporter assay system, Promega) in a GloMax® Navigator Microplate Luminometer (Promega) to measure IAV polymerase-driven Firefly luciferase activity and cellular-driven Renilla luciferase activity, respectively. Firefly luciferase values for every sample were normalised by their respective Renilla luciferase values to account for transfection efficiency variation between samples. Each sample was tested in duplicate in at least in three separate biological experiments.

MX1 and BTN3A3 susceptibility assays. For single-cycle titration of ZsGreen reporter viruses on A549-Mx1 cells, cells were cultured in 96-well plates 16 h prior to infection (1.5 x 10^4 cells/well). Cells were washed with serum-free DMEM prior to infection with 100 µL of serum-free DMEM containing serially-diluted virus. At 7 h post-infection, cells were washed with PBS and dispersed with TryLE (Gibco), resuspended in complete DMEM and fixed in 2%

formaldehyde. To measure ZsGreen-positive cells, flow cytometry was performed on a Millipore GUAVA EasyCyte HT Flow Cytometer. Percentage of ZsGreen-positive cells was determined using FlowJo (https://www.flowjo.com) software.

Immunoblotting. Total cell lysates were prepared as previously described[96]. Lysates were heated at 75 °C for 10 min and subjected to polyacrylamide gel electrophoresis before being transferred to polyvinylidene difluoride (Merck Millipore IPFL00010) membranes at 30 V for 90 min. Membranes were blocked for 1 h with 1X Tris-buffered saline-0.2% Tween 20 (TBST) containing 5% dried skimmed milk, followed by incubation with primary antibodies diluted in 5% BSA/0.01% sodium azide in 1X TBST, overnight at 4 °C. After four 10-min 1X TBST washes, membranes were incubated with secondary antibodies (diluted in blocking buffer), for 1 h at room temperature protected from direct light. Following four more washes in 1X TBST, membranes were imaged using the LI-COR CLx-Odyssey Imaging platform. The primary antibodies used in this study are: pSTAT1 (Tyr701) - Cell Signaling (9167S), RSAD2 - Proteintech (28089-1-AP), GAPDH - Cell Signaling (2118S). Mx1 antibody was kindly provided by Georg Kochs (University Medical Centre, Freiburg, Germany). Secondary antibodies used: Anti-rabbit IgG (H+L) (DyLight 800 4X PEG Conjugate) 5151S, and Anti-mouse IgG (H+L) (DyLight 680 Conjugate) 5470S.

Precision-cut bovine udder slicing and in vitro culture. Precision-cut bovine udder slices (PCBUS) were prepared from udders of commercially slaughtered dairy cows without mastitis or any antibiotic treatment. Subsequently, a piece of approximately 10cm x 10cm x 5 cm was cut out of the middle region of the bovine udder, immediately transferred into Krebs-Henseleit solution and transported to the laboratory. Tissue was cut initially into slices of roughly 1 cm, and subsequently into tissue cores with a diameter of 8 mm. To stabilize the tissue in the tissue core holder, the tissue was embedded in 3% agarose (w/v in 0.9% NaCl). PCBUS were prepared with a Krumdieck tissue slicer with a thickness of 250-350 µm. The slicer was filled with ice-cold pre-oxygenated Krebs-Henseleit solution, adjusted to a pH of 7.4. Promptly, slices were placed in a 24-well plate in 1mL of pre-warmed and pre-oxygenated medium. Incubating slices was done in RPMI-1640 medium supplemented with 1% penicillin-

streptomycin, 1% fungizone and different concentrations of FCS (0%, 2% or 10%) at 38.5°C in presence of 5% CO_2. To assess cell viability, PCBUS were examined every 24 hours until the end of the experiment using AlamarBlue®. To evaluate cell integrity, HE-staining was performed. After infection, slices were fixed in 4% formalin at 4°C for 24 h. Afterwards, slices were dehydrated in ethanol with increasing concentrations. Slices were subsequently cleared in xylene. Thereafter, slices were horizontally embedded in paraffin wax and sectioned at 2-3 µm. Prior to staining with haematoxylin and eosin (H&E), sections were deparaffinized and rehydrated. The cell viability of udder tissue was assessed by evaluating the cytoplasm and the shape/staining of nuclei as well as presence of necrosis and apoptosis.

IFN-susceptibility assays. Immortalised bovine skin fibroblasts were seeded at a density of 2.5 x 10^5 cells/well of a 24 well plate in complete DMEM media. Next day to immune prime the cells, media was removed and complete DMEM media containing a range of dilutions of Universal Type I IFN (0, 1.6, 8, 40, 200 or 1000 Units/mL; Human IFN-Alpha Hybrid Protein from PBL Assay Science, Catalog Number: 11200) were added to the cells for 24 hrs. Next Day, media was removed and cells were infected with either PR8, AIV07, Cow Texas and Human Texas viruses at a MOI of 0.001 in serum free DMEM for 1 hr at 37C. After 1h, virus was removed and virus overlay media (serum free DMEM, 0.14% fraction V BSA, 1x PenStrep, 1ug/ml TPCK Trypsin) containing same range of dilutions of Universal IFN was added for continuous immune priming of cells. Supernatant was collected at 24, 48 and 72h post infection and later used for plaque assay on MDCKs to titrate the viruses.

Mice infections. All animal work was in accordance with the animal ethics and welfare committee at the University of Glasgow and the United Kingdom Home Office regulations (ASPA, 1986, PPL PP4085778). All mice were purchased from Charles River Laboratories (United Kingdom) and housed at the CRUK Scotland Institute. Mice (male, 8 week old C57BL/6) were intranasally infected with 100 PFU of virus and monitored daily. At post-mortem, lungs were perfused and inflated with agarose, and subsequently fixed in 8 % formalin for 24 hours.

Immunohistochemistry. Formalin-fixed and paraffin embedded (FFPE) mice lung and brain tissue blocks, or precision cut udder slices were cut into ~3 µm thick sections and mounted on glass slides for immunohistochemistry (IHC) as described previously[97]. The antibodies used were anti-Influenza A H1N1 Nucleoprotein (NP; A/WSN/1933; Novus Biologicals), anti-Cluster of Differentiation 3 (CD3; Agilent Dako), anti-Paired box protein-5 (Pax-5; Abcam). To detect Mx-1, a custom-made monoclonal anti-Mx1 antibody was used (kindly provided by Georg Kochs and Hartmut Hengel, Universitaetsklinikum Freiburg, Germany). As a negative control, the primary antibody was replaced by Dako Real Antibody Diluent (Agilent Dako; Code S2022). Visualisation was performed using the Dako EnVision+ System-HRP Labelled Polymer Anti-Rabbit (Agilent Dako; code K4001) in an automated stainer (Dako Autostainer Link 48, Agilent Technologies). 3,3'-Diaminobenzidine (DAB) was used as a chromogen in all IHC experiments. For confocal imaging, the same primary antibodies (with the same concentrations) have been used as above. Secondary antibodies included AlexaFluor-488 and -594 (codes A11034, A21203; Thermo Fisher Scientific). Dapi was used for nuclear staining. Images have been captured with a Zeiss LSM 710 Confocal Microscope (Zeiss, Wetzlar, Germany).

Digital Pathology. Slides were digitised and scanned at 20x magnification using the Aperio Versa 8 Slidescanner and Aperio Versa 1.0.4.125 software (Leica Biosystems) for subsequent image analysis. Images of digitised slides were captured using the Aperio ImageScope software v12.4.3.5008 (Leica Biosystems). Positive cell detection and quantification of CD3 and Pax-5, as well as positive pixel quantification of NP, were performed using QuPath software (version 0.4.3;[98]) with settings adjusted to optimise signal detection for each marker[97]. To create the thresholder, the 'Resolution' was set to 1.09 µm/pixel or higher. For the 'Channel', we used 'DAB' (IHC); the 'Prefilter' was always 'Gaussian' while 'Smoothing sigma' as well as the 'Threshold' have been tuned for each set of experiments to optimise the correct detection. The 'Above threshold' option was always set to 'Positive' whereas the 'Below threshold' was always set to 'Negative'. The 'Region' to be analysed was set to 'Any annotation ROI'. The readout is a percentage of positive pixels per total pixels in the annotated area.

The ‘Positive cell’ detection feature has been used instead for the detection of cell membrane-associated CD3-positive cells and nucleus-localised Pax-5. The settings for the ‘Requested pixel size’ were adjusted to 0.5 µm or smaller and the ‘Nucleus parameters’ included a ‘Background radius’ of 8 µm. The ‘Median filter radius’ was set to 0.8 µm or smaller, ‘Sigma’ to 1.5 µm or smaller while the ‘Minimum’ and ‘Maximum’ areas were adjusted to 3–5 µm2 and 70-200 µm2 respectively. The ‘Intensity parameters’ included a ‘Threshold’ of 0.1 and a ‘Max. background intensity’ of 2. The ‘Cell parameters’ included a ‘Cell expansion’ of 3-4.4286 µm. The readout is a percentage of positive cells detected per all cells in the annotated area. **Statistical analysis.** Statistical analyses were performed using GraphPad Prism 10. Data were assessed for Gaussian distribution using the Shapiro-Wilk test or were Log10 transformed. Data from replication kinetics experiments were compared at each time point. Statistical significance was assessed using Brown-Forsythe and Welch’s one-way analysis of variance (ANOVA) followed by unpaired t-test with Welch correction for multiple comparison. In all analyses statistical significance was determined to be $P < 0.05$.

Acknowledgements

We thank Wendy Barclay, Paul Digard and members of the Flu:TrailMap-One Health consortium for insightful discussions. We thank Lynn Marion Stevenson, Lynn Oxford, Frazer Bell and Lewis Kidd from the Veterinary Diagnostic Service of the University of Glasgow for the excellent support with the tissue sample preparations and staining. We acknowledge funding from MRC/UKRI (Grant Ref: MR/Y03368X/1) to the to the CVR (MC_UU_00034/3, MC_UU_00034/5, MC_UU_00034/9; to M.P, P.R.M, A.D.F.). We also acknowledge the Flu:TrailMap-One Health consortium, BBSRC FLU-Trailmap (grant Ref: BB/Y007298/1) and Pirbright ISPG (grant Ref: BBS/E/PI/230001B) (to M.P, P.R.M and M.I). Additional funding was supported by CRUK core funding to the Beatson Institute (A31287) and CRUK core funding to E.W.-R. (A1920).

Table 1 – 6:2 Reassortants used in this study. Each virus has the HA and NA segments from PR8, and all remaining segments from the strain listed

Abbreviated name	Internal genes origin	Sequence details	Non-synonymous mutations detected in viral stocks
PR8	A/Puerto Rico/8/1934 (H1N1)	GenBank EF467817 to EF467824	None
r-Cow(H5N1)	A/dairy cow/Texas/24-008749-001-original/2024 (H5N1)	GISAID EPI_ISL_19014384	None
r-Tx/37(H5N1)	Human A/Texas/37/2024 (H5N1)	GISAID EPI_ISL_19027114	None
r-Goat(H5N1)	A/goat/Minnesota/24-007234-003-original/2024 (H5N1)	GISAID EPI_ISL_19015123	None
r-AIV07(H5N1)	A/chicken/England/053052/2021 (H5N1)	GISAID EPI_ISL_9012457	None
r-AIV09(H5N1)	A/chicken/Scotland/054477/2021 (H5N1)	GISAID EPI_ISL_9012696	PA D347Y
r-AIV48(H5N1)	A/chicken/England/085598/2022 (H5N1)	GISAID EPI_ISL_13782459	None
r-pdm09(H1N1)	A/California/04-061-MA/2009(H1N1)	GenBank KX134889 (PB2), MH393723.1 (PB1), MH393724.1 (PA), MH393698.1 (NP), KX136570 (M), NS: KX134783 (NS).	PA E298K, NP D101G
r-Anhui/13(H7N9)	A/Anhui/2013 (H7N9)	GISAID EPI_ISL_17264823	None
r-Eng/23(H1N2v)	A/England/2023 (H1N2v)	GISAID EPI_ISL_18548251	None
r-Canine(H3N2)	A/canine/Illinois/11613/2015 (H3N2)	doi:10.1371/journal.ppat.1008409	PA C489S
r-Equine(H3N8)	A/equine/South Africa/4/2003(H3N8)	GenBank ON797667 to ON797674	PA V51A & PA C478S

Table 2 – 4:4 Reassortants used in this study. Each virus has the HA, NA, M and NS segments from PR8, and all remaining segments from the strain listed

Abbreviated name	Internal genes origin	Sequence details
r-Mld/99(H1N1)	A/mallard/Netherlands/10-Cam/1999(H1N1)	GenBank KC209512 to KC209519
r-Cow(H5N1)	A/dairy cow/Texas/24-008749-001-original/2024 (H5N1)	GISAID EPI_ISL_19014384
r-Tx/37(H5N1)	Human A/Texas/37/2024 (H5N1)	GISAID EPI_ISL_19027114
r-Goat(H5N1)	A/goat/Minnesota/24-007234-003-original/2024 (H5N1)	GISAID EPI_ISL_19015123
r-AIV07(H5N1)	A/chicken/England/053052/2021 (H5N1)	GISAID EPI_ISL_9012457
r-AIV09(H5N1)	A/chicken/Scotland/054477/2021 (H5N1)	GISAID EPI_ISL_9012696
r-AIV48(H5N1)	A/chicken/England/085598/2022 (H5N1)	GISAID EPI_ISL_13782459
r-Eng/23(H1N2v)	A/England/2023 (H1N2v)	GISAID EPI_ISL_18548251
r-Anhui/13(H7N9)	A/Anhui/2013 (H7N9)	GISAID EPI_ISL_17264823
r-Iowa/11(H3N2v)	A/Iowa/08/2011	EPI_ISL_99214
r-Ohio/16(H3N2v)	A/Ohio/27/2016	OH/16: EPI_ISL_232044
r-Chn/23(H3N8)	A/Guangdong/ZS-2023SF005/2023	EPI_ISL_17464053
r-Arg(H4N2)	A/silver teal/Argentina/CIP051-32/2011	OQ821651.1, OQ821652.1, OQ821653.1, OQ821655.1
r-Nld(H7N7)	A/Netherlands/219/03(H7N7)	AY342413.1, AY340083.1, AY342418.1, AY342425.1
r-Chn/13(H10N8)	A/Jiangxi-Donghu/346/2013	EPI_ISL_152846

Figure Legends

Fig 1. Global phylogenies of representative IAV sequences. Maximum likelihood phylogenetic trees were constructed using IQTree software with a dataset of IAV representative sequences clustered at 0.95 identity. Annotated tips labelled with their strain names correspond to the viruses evaluated in the *in vitro* analyses. Viruses from the European and American 2.3.4.4b lineages are coloured blue and red, respectively. Trees were midpoint rooted and IAV bat viruses were pruned to improve the visualization.

Fig 2. Replication of 2.3.4.4b and B3.13 reassortant viruses *in vitro*. **a**, Madin-Darby canine kidney cells were infected with 0.0005 genome copies per cell and copies in the supernatant at each time point were determined by RT-qPCR. **b** and **c,** As above, but with bovine skin fibroblasts (**b**) and primary bovine nasal fibroblasts (**c**) that were infected with 0.001 genome copies per cell. Data are mean +/- s.d. of three independent biological experiments (n = 3). Individual points represent the mean value of two technical duplicates for each biological repeat. Data were log-transformed and confirmed to be normally distributed using the Shapiro-Wilk Test. At each timepoint, multiple comparisons between all virus titres were performed using an ordinary one-way analysis of variance (ANOVA) with Tukey's multiple comparison test (α= 0.05). Only comparisons relative to r-Tx/37(H5N1) and r-Cow(H5N1) are shown. P values in bold indicate statistical significance.

Fig 3. Polymerase activity of diverse IAV strains in human cells. a, Polymerase activity assays in HEK-293T cells at 24 h post-transfection. Data are mean +/- s.d. of three independent experiments and each data point represents the mean of two technical duplicates from each of the biological repeats. Table in (**a**) highlights in green PB2 residues that have been implicated in increased polymerase activity in previous studies[39,64,85,99-104]. **b** and **c**, The individual polymerase subunits of the r-Cow(H5N1) or r-Tx/47(H5N1) were swapped with the ancestral r-AIV07(H5N1) strain. Data are mean +/- s.d. of three independent experiments and each dot represents the mean of two technical duplicates from each of the biological repeats.

Data were log-transformed and confirmed to be normally distributed using the Shapiro-Wilk Test. Multiple comparisons between all polymerases were performed using an ordinary one-way ANOVA with Tukey's multiple comparison test (α = 0.05). Only comparisons to control polymerases are shown. P values in bold indicate statistical significance.

Fig 4. Contribution of individual B3.13-derived segments to virus replication. **a** and **b**, Bovine skin fibroblasts were infected with 6:2 viruses harbouring internal gene reassortant constellations between the ancestral r-AIV07(H5N1) strain and either r-Cow(H5N1) or r-TX/37(H5N1) strains. The PB2, PB1, NP or NS segments, or all four ('QUAD'), were swapped reciprocally between the two. Cells were infected at an MOI of 0.0001 genome copies/cell and shown are genome titres determined by RT-qPCR in the supernatant of infected cells at 24 h post-infection. Data are mean +/- s.d. of three independent experiments. Each dot represents the mean of two technical duplicates from the three biological repeats. **c** and **d**, Bovine skin fibroblasts were infected with 0.001 PFU/cell of 4:4 and 6:2 recombinant viruses. Virus in the supernatant was titrated by plaque assay on MDCK cells. Data are mean +/- s.d. of three biological repeats Data were log-transformed and confirmed to be normally distributed using the Shapiro-Wilk Test. Multiple comparisons between all reassortants were performed using an ordinary one-way ANOVA with Tukey's multiple comparison test (α = 0.05), although only comparisons relative to controls are shown. P values in bold indicate statistical significance.

Fig 5. Sensitivity of 2.3.4.4b and B3.13 reassortant viruses to type I IFN in bovine cells. Immortalised primary bovine fibroblasts were pre-treated for 24 h with increasing concentrations of type I IFN prior to a low MOI (0.001 PFU/cell) infection. **a**, Western blotting for interferon-stimulated genes pSTAT1, Mx1, and RSAD2 at 24 h post IFN-treatment. **b**, virus in the supernatant of infected cells were titrated by plaque assay on MDCK cells at indicated timepoint post-infection. Data are from three biological repeats and plotted are the titres from each experiment as mean +/- s.d. Data were log-transformed and the statistical significances between IFN treatmented and untreated viruses within each group were measured by two-

way ANOVA with Dunnett's multiple comparisons tests (α = 0.05). P values in bold indicate statistical significance. **c** and **d**, Udder slices infected with r-Tx/37/(H5N1) with 10^6 genome copies/slice of tissue. Staining for NP in the duct of udder slices as brown signal in the epithelium and cells detaching from the epithelium. Mx-1 signal is located in the cytoplasm of duct epithelium of udder slices. Confocal images of udder slices with staining for NP and Mx-1 show little colocalization of the signal (merged) in the duct epithelium of infected udder slices. Bars, 100 μm (**c**) and 20 μm (**d**).

Fig 6. Effect of MX1 and BTN3A3 on 2.3.4.4b and B3.13-derived reassortant viruses *in vitro.* **a**, Western blotting of cell lysates obtained from A549 and bovine skin fibroblasts stably expressing human MX1 (MXA), and bovine, chicken and rat MX1. **b,** Single-cycle titration of ZsGreen-expressing reporter viruses on modified A549 cells. Cells were infected for 7 h and percentage of ZsGreen cells measured by flow cytometry. Plotted are titres relative to Chicken MX1 control cells. **c,** Modified A549 cells overexpressing MX1 were infected at MOI 0.001 (Pfu/cell) and infectious titre in the supernatant at 48h was determined by plaque assay on MDCK. **d,** Modified bovine skin fibroblasts overexpressing MX1 were infected at an MOI of 0.001 (Pfu/cell) and infectious titres in the supernatant at 24 hpi were determined by plaque assay on MDCK cells. **e**, As described in (**d**) except recombinant 4:4 viruses (Table 2) were used and peak titre of each virus (either 24h or 48h) is shown. **f**, Western blotting of lysates from MDCK cells overexpressing human BTN3A3. **g**, Titres on modified MDCK cells overexpressing human BTN3A3 or transduced with a control empty vector. The experiments described are from three biological repeats, except for (**d**), which are from four repeats. Data in **(c-g)** were log-transformed and statistical significances between groups in each experiment were measured by two-way ANOVA with Dunnett's multiple comparisons tests (b-d, g), or Holm–Šídák test (e). Only comparisons relative to untreated or chicken MX1 controls are shown. P values in bold indicate statistical significance.

Fig 7. Virulence of 2.3.4.4b and B3.13-derived reassortants in an experimental mouse model. Groups of 10 BALB/c mice were infected with 100 PFU of each recombinant virus, or

mock-infected with PBS. 5 mice were euthanized at day 3 and the remaining 5 mice at day 8. **a**, Weights were measured daily. **b** to **d**, Within the lung the amount of viral protein (NP, **b**), the numbers of B cells (CD3, **c**) or T cells (Pax-5, **d**), respectively, was quantified in whole scanned slides of FFPE lung sections and calculated as positive pixel (NP, **b**) or positive cells (CD3, **c**; Pax-5, **d**) per lung area. **e**, Immunohistochemistry of lung sections collected from mock-infected and infected mice (r-AIV07(H5N1), r-cow(H5N1) and PR8, respectively, showing virus positive cells (NP) with brown signal in the bronchi and in the parenchyma (bar, 200 μm). In **b)** Statistical significance was determined using a repeated measures two-way ANOVA with Tukey's multiple comparison test (α= 0.05). Data in **c)** and **d)** were confirmed to be normally distributed using the Shapiro-Wilk Test and an ordinary one-way ANOVA with Tukey's multiple comparison test (α = 0.05) was used to compare groups.

Supplemental Figure Legends

Fig S1. Replication of 2.3.4.4b and B3.13 reassortant viruses in bovine epithelial cells and lung explants. **a**, Bovine mammary epithelial cells were infected with 0.001 genome copies per cell and copies in the supernatant at shown timepoint was determined by RT-qPCR. Data are mean +/- s.d. of three independent biological experiments (n = 3). Individual points represent the mean value of two technical duplicates for each biological repeat. Data were log-transformed and confirmed to be normally distributed with equal variance using Brown-Forsyth and Bartlett's tests, $p > 0.05$. At each time point, multiple comparisons between all virus titres were performed using an ordinary one-way analysis of variance (ANOVA) with Tukey's multiple comparison test (α = 0.05). P values in bold are significant. **b**, Representative images of uninfected histological sections stained with haematoxylin and eosin of bovine bronchial epithelium from post-mortem material (i), and at day 1 (ii), 2 (iii) , and 3 (iv) post-culture under air-liquid interface conditions. All images are shown at 20x magnification.

Fig S2. Comparison of qPCR- and PFU-based virus titration methods. Bovine nasal fibroblasts were infected with 0.001 genome copies per cell and infectious titers and genomic copies in the supernatant at 24 hours post infection were titrated by plaque assay on MDCK

cells or by RT-qPCR, respectively, on the same supernatant samples. Data are mean +/- s.d. of three independent biological experiments (n = 3). Individual points represent the mean value of two technical duplicates for each biological repeat. Data were log-transformed and confirmed to be normally distributed using the Shapiro-Wilk Test. Multiple comparisons between all reassortants were performed using an ordinary one-way ANOVA with Tukey's multiple comparison test (α = 0.05), although only comparisons relative to controls are shown. P values in bold indicate statistical significance.

References

1 Chambers, T. M. Equine Influenza. *Cold Spring Harb Perspect Med* **12** (2022). https://doi.org:10.1101/cshperspect.a038331

2 Vincent, A. *et al.* Review of influenza A virus in swine worldwide: a call for increased surveillance and research. *Zoonoses Public Health* **61**, 4-17 (2014). https://doi.org:10.1111/zph.12049

3 Wasik, B. R., Voorhees, I. E. H. & Parrish, C. R. Canine and Feline Influenza. *Cold Spring Harb Perspect Med* **11** (2021). https://doi.org:10.1101/cshperspect.a038562

4 Gass, J. D., Jr. *et al.* Epidemiology and Ecology of Influenza A Viruses among Wildlife in the Arctic. *Viruses* **14** (2022). https://doi.org:10.3390/v14071531

5 Fereidouni, S. *et al.* Genetic characterization of a new candidate hemagglutinin subtype of influenza A viruses. *Emerg Microbes Infect* **12**, 2225645 (2023). https://doi.org:10.1080/22221751.2023.2225645

6 Worobey, M., Han, G. Z. & Rambaut, A. Genesis and pathogenesis of the 1918 pandemic H1N1 influenza A virus. *Proc Natl Acad Sci U S A* **111**, 8107-8112 (2014). https://doi.org:10.1073/pnas.1324197111

7 Scholtissek, C., Rohde, W., Von Hoyningen, V. & Rott, R. On the origin of the human influenza virus subtypes H2N2 and H3N2. *Virology* **87**, 13-20 (1978).

8 Kawaoka, Y., Krauss, S. & Webster, R. G. Avian-to-human transmission of the PB1 gene of influenza A viruses in the 1957 and 1968 pandemics. *J Virol* **63**, 4603-4608 (1989). https://doi.org:10.1128/jvi.63.11.4603-4608.1989

9 Taubenberger, J. K. *et al.* Characterization of the 1918 influenza virus polymerase genes. *Nature* **437**, 889-893 (2005). https://doi.org:http://www.nature.com/nature/journal/v437/n7060/suppinfo/nature04230_S1.html

10 Patrono, L. V. *et al.* Archival influenza virus genomes from Europe reveal genomic variability during the 1918 pandemic. *Nat Commun* **13**, 2314 (2022). https://doi.org:10.1038/s41467-022-29614-9

11 Peacock, T. *et al.* The global H5N1 influenza panzootic in mammals. *Nature* (2024). https://doi.org:10.1038/s41586-024-08054-z

12 Pohlmann, A. *et al.* Has epizootic become enzootic? Evidence for a fundamental change in the infection dynamics of highly pathogenic avian influenza in Europe, 2021. *MBio* **13**, e00609-00622 (2022).

13 Caliendo, V. *et al.* Transatlantic spread of highly pathogenic avian influenza H5N1 by wild birds from Europe to North America in 2021. *Scientific reports* **12**, 11729 (2022).

14 Elsmo, E. J. *et al.* Highly Pathogenic Avian Influenza A(H5N1) Virus Clade 2.3.4.4b Infections in Wild Terrestrial Mammals, United States, 2022. *Emerg Infect Dis* **29**, 2451-2460 (2023). https://doi.org:10.3201/eid2912.230464

15 Jakobek, B. T. *et al.* Influenza A(H5N1) Virus Infections in 2 Free-Ranging Black Bears (Ursus americanus), Quebec, Canada. *Emerg Infect Dis* **29**, 2145-2149 (2023). https://doi.org:10.3201/eid2910.230548

16 Moreno, A. *et al.* Asymptomatic infection with clade 2.3.4.4b highly pathogenic avian influenza A(H5N1) in carnivore pets, Italy, April 2023. *Euro Surveill* **28** (2023). https://doi.org:10.2807/1560-7917.ES.2023.28.35.2300441

17 Rabalski, L. *et al.* Emergence and potential transmission route of avian influenza A (H5N1) virus in domestic cats in Poland, June 2023. *Euro Surveill* **28** (2023). https://doi.org:10.2807/1560-7917.ES.2023.28.31.2300390

18 Leguia, M. *et al.* Highly pathogenic avian influenza A (H5N1) in marine mammals and seabirds in Peru. *Nature Communications* **14**, 5489 (2023). https://doi.org:10.1038/s41467-023-41182-0

19 Pardo-Roa, C. *et al.* Cross-species transmission and PB2 mammalian adaptations of highly pathogenic avian influenza A/H5N1 viruses in Chile. *bioRxiv* (2023). https://doi.org:10.1101/2023.06.30.547205

20 Uhart, M. *et al.* Massive outbreak of Influenza A H5N1 in elephant seals at Península Valdés, Argentina: increased evidence for mammal-to-mammal transmission. *bioRxiv*, 2024.2005.2031.596774 (2024). https://doi.org:10.1101/2024.05.31.596774
21 Tomás, G. *et al.* Highly pathogenic avian influenza H5N1 virus infections in pinnipeds and seabirds in Uruguay: Implications for bird-mammal transmission in South America. *Virus Evol* **10**, veae031 (2024). https://doi.org:10.1093/ve/veae031
22 Burrough, E. R. *et al.* Highly Pathogenic Avian Influenza A(H5N1) Clade 2.3.4.4b Virus Infection in Domestic Dairy Cattle and Cats, United States, 2024. *Emerg Infect Dis* **30** (2024). https://doi.org:10.3201/eid3007.240508
23 Caliendo, V. *et al.* Transatlantic spread of highly pathogenic avian influenza H5N1 by wild birds from Europe to North America in 2021. *Scientific Reports* **12**, 11729 (2022). https://doi.org:10.1038/s41598-022-13447-z
24 Caserta, L. C. *et al.* Spillover of highly pathogenic avian influenza H5N1 virus to dairy cattle. *Nature* **634**, 669-676 (2024). https://doi.org:10.1038/s41586-024-07849-4
https://virological.org/t/preliminary-report-on-genomic-epidemiology-of-the-2024-h5n1-influenza-a-virus-outbreak-in-u-s-cattle-part-1-of-2/970/126 Nguyen, T.-Q. *et al.* Emergence and interstate spread of highly pathogenic avian influenza A(H5N1) in dairy cattle. *bioRxiv*, 2024.2005.2001.591751 (2024). https://doi.org:10.1101/2024.05.01.591751
27 Kalthoff, D., Hoffmann, B., Harder, T., Durban, M. & Beer, M. Experimental infection of cattle with highly pathogenic avian influenza virus (H5N1). *Emerg Infect Dis* **14**, 1132-1134 (2008). https://doi.org:10.3201/eid1407.071468
28 Sreenivasan, C. C., Thomas, M., Kaushik, R. S., Wang, D. & Li, F. Influenza A in Bovine Species: A Narrative Literature Review. *Viruses* **11** (2019). https://doi.org:10.3390/v11060561
https://www.cdc.gov/bird-flu/situation-summary/index.html?CDC_AA_refVal=https%3A%2F%2Fwww.cdc.gov%2Fbird-flu%2Fphp%2Favian-flu-summary%2Findex.html30 APHIS. *H5N1 Highly Pathogenic Avian Influenza (HPAI) in Livestock: Information for small ruminant (sheep and goat) and camelid stakeholders* <https://www.aphis.usda.gov/sites/default/files/small-ruminant-camelid-h5n1-info.pdf> (2024).
31 Long, J. S., Mistry, B., Haslam, S. M. & Barclay, W. S. Host and viral determinants of influenza A virus species specificity. *Nature Reviews Microbiology* **17**, 67-81 (2019). https://doi.org:10.1038/s41579-018-0115-z
32 Gagneux, P. *et al.* Human-specific Regulation of α2–6-linked Sialic Acids*. *Journal of Biological Chemistry* **278**, 48245-48250 (2003). https://doi.org:https://doi.org/10.1074/jbc.M309813200
33 Shinya, K. *et al.* Avian flu: influenza virus receptors in the human airway. *Nature* **440**, 435-436 (2006). https://doi.org:10.1038/440435a
34 Fukuyama, S. *et al.* Multi-spectral fluorescent reporter influenza viruses (Color-flu) as powerful tools for in vivo studies. *Nat Commun* **6**, 6600 (2015). https://doi.org:10.1038/ncomms7600
35 Matrosovich, M. N., Matrosovich, T. Y., Gray, T., Roberts, N. A. & Klenk, H. D. Human and avian influenza viruses target different cell types in cultures of human airway epithelium. *Proc Natl Acad Sci U S A* **101**, 4620-4624 (2004). https://doi.org:10.1073/pnas.0308001101
36 van Riel, D. *et al.* H5N1 Virus Attachment to Lower Respiratory Tract. *Science* **312**, 399-399 (2006). https://doi.org:10.1126/science.1125548
37 Russell, C. J., Hu, M. & Okda, F. A. Influenza Hemagglutinin Protein Stability, Activation, and Pandemic Risk. *Trends Microbiol* **26**, 841-853 (2018). https://doi.org:10.1016/j.tim.2018.03.005
38 Blumenkrantz, D., Roberts, K. L., Shelton, H., Lycett, S. & Barclay, W. S. The short stalk length of highly pathogenic avian influenza H5N1 virus neuraminidase limits transmission of pandemic H1N1 virus in ferrets. *J Virol* **87**, 10539-10551 (2013). https://doi.org:10.1128/jvi.00967-13

39 Long, J. S. *et al.* Species difference in ANP32A underlies influenza A virus polymerase host restriction. *Nature* **529**, 101-104 (2016). https://doi.org:10.1038/nature16474
40 Zhang, H. *et al.* Fundamental Contribution and Host Range Determination of ANP32A and ANP32B in Influenza A Virus Polymerase Activity. *J Virol* **93** (2019). https://doi.org:10.1128/jvi.00174-19
41 Long, J. S. *et al.* Species specific differences in use of ANP32 proteins by influenza A virus. *Elife* **8** (2019). https://doi.org:10.7554/eLife.45066
42 Staller, E. *et al.* ANP32 Proteins Are Essential for Influenza Virus Replication in Human Cells. *J Virol* **93** (2019). https://doi.org:10.1128/jvi.00217-19
43 Zhang, Z. *et al.* Selective usage of ANP32 proteins by influenza B virus polymerase: Implications in determination of host range. *PLOS Pathogens* **16**, e1008989 (2020). https://doi.org:10.1371/journal.ppat.1008989
44 Carrique, L. *et al.* Host ANP32A mediates the assembly of the influenza virus replicase. *Nature* **587**, 638-643 (2020). https://doi.org:10.1038/s41586-020-2927-z
45 Gabriel, G. *et al.* Differential use of importin-α isoforms governs cell tropism and host adaptation of influenza virus. *Nature Communications* **2**, 156 (2011). https://doi.org:10.1038/ncomms1158
46 Pinto, R. M. *et al.* BTN3A3 evasion promotes the zoonotic potential of influenza A viruses. *Nature* **619**, 338-347 (2023). https://doi.org:10.1038/s41586-023-06261-8
47 Dittmann, J. *et al.* Influenza A virus strains differ in sensitivity to the antiviral action of Mx-GTPase. *J Virol* **82**, 3624-3631 (2008). https://doi.org:10.1128/jvi.01753-07
48 Zimmermann, P., Manz, B., Haller, O., Schwemmle, M. & Kochs, G. The viral nucleoprotein determines Mx sensitivity of influenza A viruses. *J Virol* **85**, 8133-8140 (2011). https://doi.org:10.1128/jvi.00712-11
49 Mänz, B. *et al.* Pandemic Influenza A Viruses Escape from Restriction by Human MxA through Adaptive Mutations in the Nucleoprotein. *PLOS Pathogens* **9**, e1003279 (2013). https://doi.org:10.1371/journal.ppat.1003279
50 Deeg, C. M. *et al.* In vivo evasion of MxA by avian influenza viruses requires human signature in the viral nucleoprotein. *J Exp Med* **214**, 1239-1248 (2017). https://doi.org:10.1084/jem.20161033
51 Haller, O. & Kochs, G. Mx genes: host determinants controlling influenza virus infection and trans-species transmission. *Hum Genet* **139**, 695-705 (2020). https://doi.org:10.1007/s00439-019-02092-8
52 Cauldwell, A. V., Long, J. S., Moncorge, O. & Barclay, W. S. Viral determinants of influenza A virus host range. *J Gen Virol* **95**, 1193-1210 (2014). https://doi.org:10.1099/vir.0.062836-0
53 Turnbull, M. L. *et al.* Role of the B Allele of Influenza A Virus Segment 8 in Setting Mammalian Host Range and Pathogenicity. *J Virol* **90**, 9263-9284 (2016). https://doi.org:10.1128/JVI.01205-16
54 Nations, F. a. A. O. o. t. U. *Livestock Systems*, <https://www.fao.org/livestock-systems/global-distributions/cattle/en/> (2024).
55 Eisfeld, A. J. *et al.* Pathogenicity and transmissibility of bovine H5N1 influenza virus. *Nature* (2024). https://doi.org:10.1038/s41586-024-07766-6
56 Santos, J. J. S. *et al.* Bovine H5N1 influenza virus binds poorly to human-type sialic acid receptors. *bioRxiv* (2024). https://doi.org:10.1101/2024.08.01.606177
57 Chopra, P. *et al.* Receptor Binding Specificity of a Bovine A(H5N1) Influenza Virus. *bioRxiv* (2024). https://doi.org:10.1101/2024.07.30.605893
58 Yang, J. *et al.* The Haemagglutinin Gene of Bovine Origin H5N1 Influenza Viruses Currently Retains an Avian Influenza Virus phenotype. *bioRxiv*, 2024.2009.2027.615407 (2024). https://doi.org:10.1101/2024.09.27.615407
59 Kristensen, C., Jensen, H. E., Trebbien, R., Webby, R. J. & Larsen, L. E. Avian and Human Influenza A Virus Receptors in Bovine Mammary Gland. *Emerg Infect Dis* **30**, 1907-1911 (2024). https://doi.org:10.3201/eid3009.240696
60 Ríos Carrasco, M., Gröne, A., van den Brand, J. M. A. & de Vries, R. P. The mammary glands of cows abundantly display receptors for circulating avian H5 viruses. *J Virol*, e0105224 (2024). https://doi.org:10.1128/jvi.01052-24

61 Bourret, V. *et al.* Whole-genome, deep pyrosequencing analysis of a duck influenza A virus evolution in swine cells. *Infection, Genetics and Evolution* **18**, 31-41 (2013). https://doi.org:https://doi.org/10.1016/j.meegid.2013.04.034
62 Zavizion, B., van Duffelen, M., Schaeffer, W. & Politis, I. Establishment and characterization of a bovine mammary epithelial cell line with unique properties. *In Vitro Cell Dev Biol Anim* **32**, 138-148 (1996). https://doi.org:10.1007/bf02723679
63 Hardy, A. *et al.* The Timing and Magnitude of the Type I Interferon Response Are Correlated with Disease Tolerance in Arbovirus Infection. *mBio* **14**, e0010123 (2023). https://doi.org:10.1128/mbio.00101-23
64 Zhang, X. *et al.* Enhanced pathogenicity and neurotropism of mouse-adapted H10N7 influenza virus are mediated by novel PB2 and NA mutations. *Journal of General Virology* **98**, 1185-1195 (2017). https://doi.org:https://doi.org/10.1099/jgv.0.000770
65 Zhang, X. *et al.* Enhanced pathogenicity and neurotropism of mouse-adapted H10N7 influenza virus are mediated by novel PB2 and NA mutations. *J Gen Virol* **98**, 1185-1195 (2017). https://doi.org:10.1099/jgv.0.000770
66 Schoggins, J. W. Interferon-Stimulated Genes: What Do They All Do? *Annu Rev Virol* **6**, 567-584 (2019). https://doi.org:10.1146/annurev-virology-092818-015756
67 Schoggins, J. W. *et al.* A diverse range of gene products are effectors of the type I interferon antiviral response. *Nature* **472**, 481-485 (2011). https://doi.org:10.1038/nature09907
68 Shaw, A. E. *et al.* Fundamental properties of the mammalian innate immune system revealed by multispecies comparison of type I interferon responses. *PLOS Biology* **15**, e2004086 (2017). https://doi.org:10.1371/journal.pbio.2004086
69 Halwe, N. J. *et al.* H5N1 clade 2.3.4.4b dynamics in experimentally infected calves and cows. *Nature* (2024). https://doi.org:10.1038/s41586-024-08063-y
70 Briggs, K., Chrzastek, K., Segovia, K., Mo, J. & Kapczynski, D. R. Genetic insertion of mouse Myxovirus-resistance gene 1 increases innate resistance against both high and low pathogenic avian influenza virus by significantly decreasing replication in chicken DF1 cell line. *Virology* **595**, 110066 (2024). https://doi.org:https://doi.org/10.1016/j.virol.2024.110066
71 Wang, Y. *et al.* Associations of chicken Mx1 polymorphism with antiviral responses in avian influenza virus infected embryos and broilers. *Poultry Science* **91**, 3019-3024 (2012). https://doi.org:https://doi.org/10.3382/ps.2012-02471
72 Schusser, B. *et al.* Mx Is Dispensable for Interferon-Mediated Resistance of Chicken Cells against Influenza A Virus. *Journal of Virology* **85**, 8307-8315 (2011). https://doi.org:doi:10.1128/jvi.00535-11
73 Arnheiter, H. & Haller, O. Antiviral state against influenza virus neutralized by microinjection of antibodies to interferon-induced Mx proteins. *Embo j* **7**, 1315-1320 (1988). https://doi.org:10.1002/j.1460-2075.1988.tb02946.x
74 Bouvier, N. M. & Lowen, A. C. Animal Models for Influenza Virus Pathogenesis and Transmission. *Viruses* **2**, 1530-1563 (2010). https://doi.org:10.3390/v20801530
75 Hatta, M., Gao, P., Halfmann, P. & Kawaoka, Y. Molecular basis for high virulence of Hong Kong H5N1 influenza A viruses. *Science* **293**, 1840-1842 (2001). https://doi.org:10.1126/science.1062882
76 Schrauwen, E. J. *et al.* The multibasic cleavage site in H5N1 virus is critical for systemic spread along the olfactory and hematogenous routes in ferrets. *J Virol* **86**, 3975-3984 (2012). https://doi.org:10.1128/jvi.06828-11
77 Pensaert, M., Ottis, K., Vandeputte, J., Kaplan, M. M. & Bachmann, P. A. Evidence for the natural transmission of influenza A virus from wild ducks to swine and its potential importance for man. *Bull World Health Organ* **59**, 75-78 (1981).
78 Webster, R. G. Are equine 1 influenza viruses still present in horses? *Equine Vet J* **25**, 537-538 (1993). https://doi.org:10.1111/j.2042-3306.1993.tb03009.x
79 Waddell, G. H., Teigland, M. B. & Sigel, M. M. A NEW INFLUENZA VIRUS ASSOCIATED WITH EQUINE RESPIRATORY DISEASE. *J Am Vet Med Assoc* **143**, 587-590 (1963).

80 Guo, Y. *et al.* Characterization of a new avian-like influenza A virus from horses in China. *Virology* **188**, 245-255 (1992).
81 Zhu, H., Hughes, J. & Murcia, P. R. Origins and Evolutionary Dynamics of H3N2 Canine Influenza Virus. *Journal of virology* **89**, 5406-5418 (2015). https://doi.org:10.1128/jvi.03395-14
82 Worobey, M., Han, G.-Z. & Rambaut, A. A synchronized global sweep of the internal genes of modern avian influenza virus. *Nature* **508**, 254-257 (2014). https://doi.org:10.1038/nature13016
83 Agüero, M. *et al.* Highly pathogenic avian influenza A(H5N1) virus infection in farmed minks, Spain, October 2022. *Euro Surveill* **28** (2023). https://doi.org:10.2807/1560-7917.Es.2023.28.3.2300001
84 Uhart, M. M. *et al.* Epidemiological data of an influenza A/H5N1 outbreak in elephant seals in Argentina indicates mammal-to-mammal transmission. *Nature Communications* **15**, 9516 (2024). https://doi.org:10.1038/s41467-024-53766-5
85 Subbarao, E. K., London, W. & Murphy, B. R. A single amino acid in the PB2 gene of influenza A virus is a determinant of host range. *J Virol* **67**, 1761-1764 (1993). https://doi.org:10.1128/jvi.67.4.1761-1764.1993
86 Yamayoshi, S. *et al.* Enhanced Replication of Highly Pathogenic Influenza A(H7N9) Virus in Humans. *Emerg Infect Dis* **24**, 746-750 (2018). https://doi.org:10.3201/eid2404.171509
87 Gu, C. *et al.* A human isolate of bovine H5N1 is transmissible and lethal in animal models. *Nature* (2024). https://doi.org:10.1038/s41586-024-08254-7
88 Gilbertson, B. & Subbarao, K. Mammalian infections with highly pathogenic avian influenza viruses renew concerns of pandemic potential. *Journal of Experimental Medicine* **220** (2023). https://doi.org:10.1084/jem.20230447
89 Steinegger, M. & Söding, J. MMseqs2 enables sensitive protein sequence searching for the analysis of massive data sets. *Nat Biotechnol* **35**, 1026-1028 (2017). https://doi.org:10.1038/nbt.3988
90 Katoh, K. & Standley, D. M. MAFFT Multiple Sequence Alignment Software Version 7: Improvements in Performance and Usability. *Molecular Biology and Evolution* **30**, 772-780 (2013). https://doi.org:10.1093/molbev/mst010
91 Minh, B. Q. *et al.* IQ-TREE 2: New Models and Efficient Methods for Phylogenetic Inference in the Genomic Era. *Mol Biol Evol* **37**, 1530-1534 (2020). https://doi.org:10.1093/molbev/msaa015
92 Yu, G., Smith, D. K., Zhu, H., Guan, Y. & Lam, T. T.-Y. ggtree: an r package for visualization and annotation of phylogenetic trees with their covariates and other associated data. *Methods in Ecology and Evolution* **8**, 28-36 (2017). https://doi.org:https://doi.org/10.1111/2041-210X.12628
93 Hardy, A. *et al.* The Timing and Magnitude of the Type I Interferon Response Are Correlated with Disease Tolerance in Arbovirus Infection. *mBio* **14**, e00101-00123 (2023). https://doi.org:doi:10.1128/mbio.00101-23
94 Rihn, S. J. *et al.* A plasmid DNA-launched SARS-CoV-2 reverse genetics system and coronavirus toolkit for COVID-19 research. *PLOS Biology* **19**, e3001091 (2021). https://doi.org:10.1371/journal.pbio.3001091
95 Hoffmann, E., Stech, J., Guan, Y., Webster, R. G. & Perez, D. R. Universal primer set for the full-length amplification of all influenza A viruses. *Arch Virol* **146**, 2275-2289 (2001).
96 Bakshi, S., Taylor, J., Strickson, S., McCartney, T. & Cohen, P. Identification of TBK1 complexes required for the phosphorylation of IRF3 and the production of interferon β. *Biochem J* **474**, 1163-1174 (2017). https://doi.org:10.1042/bcj20160992
97 Meehan, G. R. *et al.* Phenotyping the virulence of SARS-CoV-2 variants in hamsters by digital pathology and machine learning. *PLOS Pathogens* **19**, e1011589 (2023). https://doi.org:10.1371/journal.ppat.1011589
98 Bankhead, P. *et al.* QuPath: Open source software for digital pathology image analysis. *Scientific Reports* **7**, 16878 (2017). https://doi.org:10.1038/s41598-017-17204-5

99 Yamada, S. *et al.* Biological and Structural Characterization of a Host-Adapting Amino Acid in Influenza Virus. *PLoS Pathog* **6**, e1001034 (2010). https://doi.org:10.1371/journal.ppat.1001034

100 Bussey, K. A., Bousse, T. L., Desmet, E. A., Kim, B. & Takimoto, T. PB2 Residue 271 Plays a Key Role in Enhanced Polymerase Activity of Influenza A Viruses in Mammalian Host Cells. *Journal of Virology* **84**, 4395-4406 (2010). https://doi.org:doi:10.1128/jvi.02642-09

101 Fan, S. *et al.* Novel residues in avian influenza virus PB2 protein affect virulence in mammalian hosts. *Nature Communications* **5**, 5021 (2014). https://doi.org:10.1038/ncomms6021

102 Steel, J., Lowen, A. C., Mubareka, S. & Palese, P. Transmission of Influenza Virus in a Mammalian Host Is Increased by PB2 Amino Acids 627K or 627E/701N. *PLoS Pathog* **5**, e1000252 (2009). https://doi.org:10.1371/journal.ppat.1000252

103 Zhou, B. *et al.* Asparagine Substitution at PB2 Residue 701 Enhances the Replication, Pathogenicity, and Transmission of the 2009 Pandemic H1N1 Influenza A Virus. *PLOS ONE* **8**, e67616 (2013). https://doi.org:10.1371/journal.pone.0067616

104 Peacock, T. P. *et al.* Mammalian ANP32A and ANP32B Proteins Drive Differential Polymerase Adaptations in Avian Influenza Virus. *Journal of Virology* **97**, e00213-00223 (2023). https://doi.org:doi:10.1128/jvi.00213-23

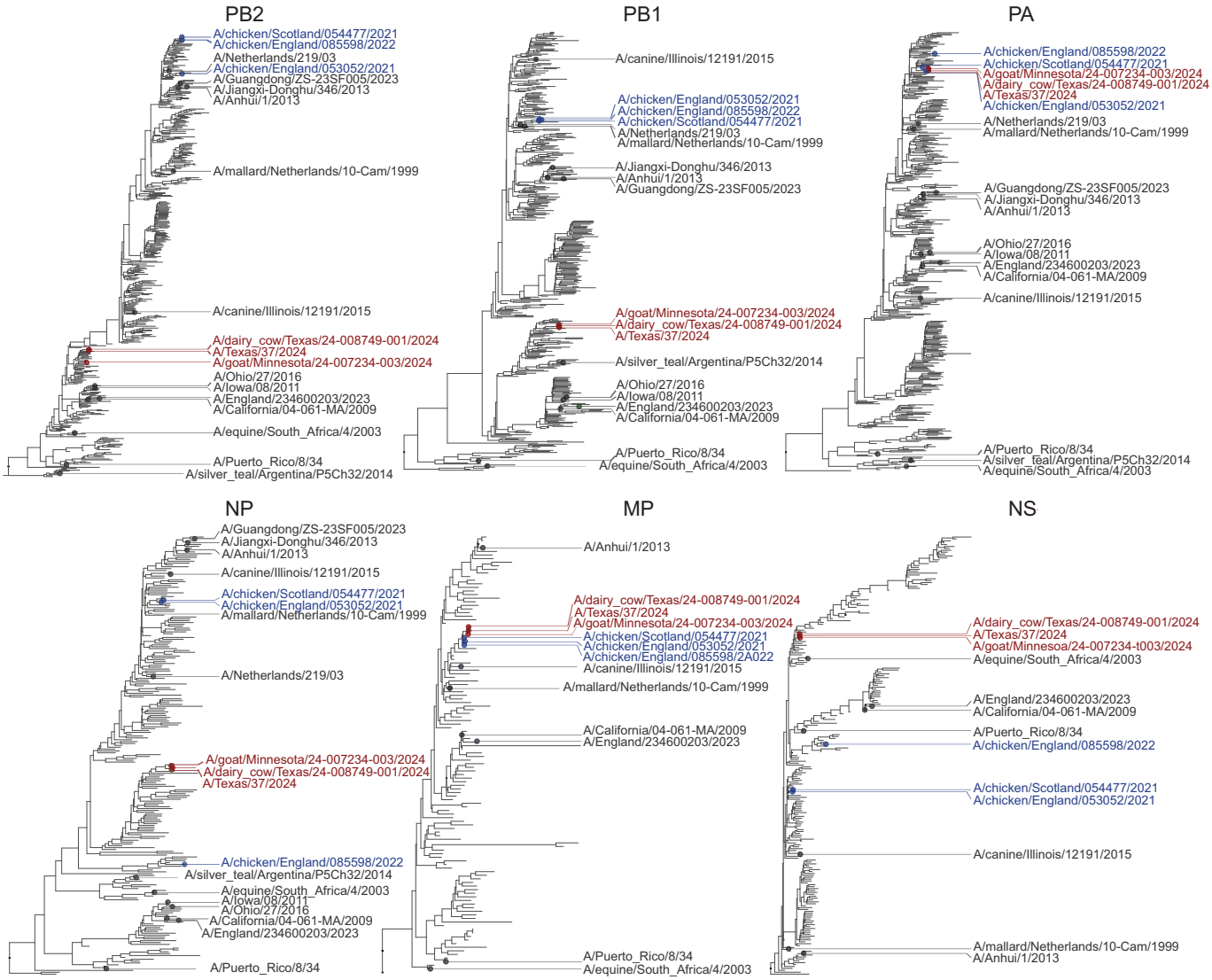
PB2
A/chicken/Scotland/054477/2021
A/chicken/England/085598/2022
A/Netherlands/219/03
A/chicken/England/053052/2021
A/Guangdong/ZS-23SF005/2023
A/Jiangxi-Donghu/346/2013
A/Anhui/1/2013
A/mallard/Netherlands/10-Cam/1999
A/canine/Illinois/12191/2015
A/dairy_cow/Texas/24-008749-001/2024
A/Texas/37/2024
A/goat/Minnesota/24-007234-003/2024
A/Ohio/27/2016
A/Iowa/08/2011
A/England/234600203/2023
A/California/04-061-MA/2009
A/equine/South_Africa/4/2003
A/Puerto_Rico/8/34
A/silver_teal/Argentina/P5Ch32/2014
PB1
A/canine/Illinois/12191/2015
A/chicken/England/053052/2021
A/chicken/England/085598/2022
A/chicken/Scotland/054477/2021
A/Netherlands/219/03
A/mallard/Netherlands/10-Cam/1999
A/Jiangxi-Donghu/346/2013
A/Anhui/1/2013
A/Guangdong/ZS-23SF005/2023
A/goat/Minnesota/24-007234-003/2024
A/dairy_cow/Texas/24-008749-001/2024
A/Texas/37/2024
A/silver_teal/Argentina/P5Ch32/2014
A/Ohio/27/2016
A/Iowa/08/2011
A/England/234600203/2023
A/California/04-061-MA/2009
A/Puerto_Rico/8/34
A/equine/South_Africa/4/2003
PA
A/chicken/England/085598/2022
A/chicken/Scotland/054477/2021
A/goat/Minnesota/24-007234-003/2024
A/dairy_cow/Texas/24-008749-001/2024
A/Texas/37/2024
A/chicken/England/053052/2021
A/Netherlands/219/03
A/mallard/Netherlands/10-Cam/1999
A/Guangdong/ZS-23SF005/2023
A/Jiangxi-Donghu/346/2013
A/Anhui/1/2013
A/Ohio/27/2016
A/Iowa/08/2011
A/England/234600203/2023
A/California/04-061-MA/2009
A/canine/Illinois/12191/2015
A/Puerto_Rico/8/34
A/silver_teal/Argentina/P5Ch32/2014
A/equine/South_Africa/4/2003
NP
A/Guangdong/ZS-23SF005/2023
A/Jiangxi-Donghu/346/2013
A/Anhui/1/2013
A/canine/Illinois/12191/2015
A/chicken/Scotland/054477/2021
A/chicken/England/053052/2021
A/mallard/Netherlands/10-Cam/1999
A/Netherlands/219/03
A/goat/Minnesota/24-007234-003/2024
A/dairy_cow/Texas/24-008749-001/2024
A/Texas/37/2024
A/chicken/England/085598/2022
A/silver_teal/Argentina/P5Ch32/2014
A/equine/South_Africa/4/2003
A/Iowa/08/2011
A/Ohio/27/2016
A/California/04-061-MA/2009
A/England/234600203/2023
A/Puerto_Rico/8/34
MP
A/Anhui/1/2013
A/dairy_cow/Texas/24-008749-001/2024
A/Texas/37/2024
A/goat/Minnesota/24-007234-003/2024
A/chicken/Scotland/054477/2021
A/chicken/England/053052/2021
A/chicken/England/085598/2A022
A/canine/Illinois/12191/2015
A/mallard/Netherlands/10-Cam/1999
A/California/04-061-MA/2009
A/England/234600203/2023
A/Puerto_Rico/8/34
A/equine/South_Africa/4/2003
NS
A/dairy_cow/Texas/24-008749-001/2024
A/Texas/37/2024
A/goat/Minnesoa/24-007234-t003/2024
A/equine/South_Africa/4/2003
A/England/234600203/2023
A/California/04-061-MA/2009
A/Puerto_Rico/8/34
A/chicken/England/085598/2022
A/chicken/Scotland/054477/2021
A/chicken/England/053052/2021
A/canine/Illinois/12191/2015
A/mallard/Netherlands/10-Cam/1999
A/Anhui/1/2013

Fig 1

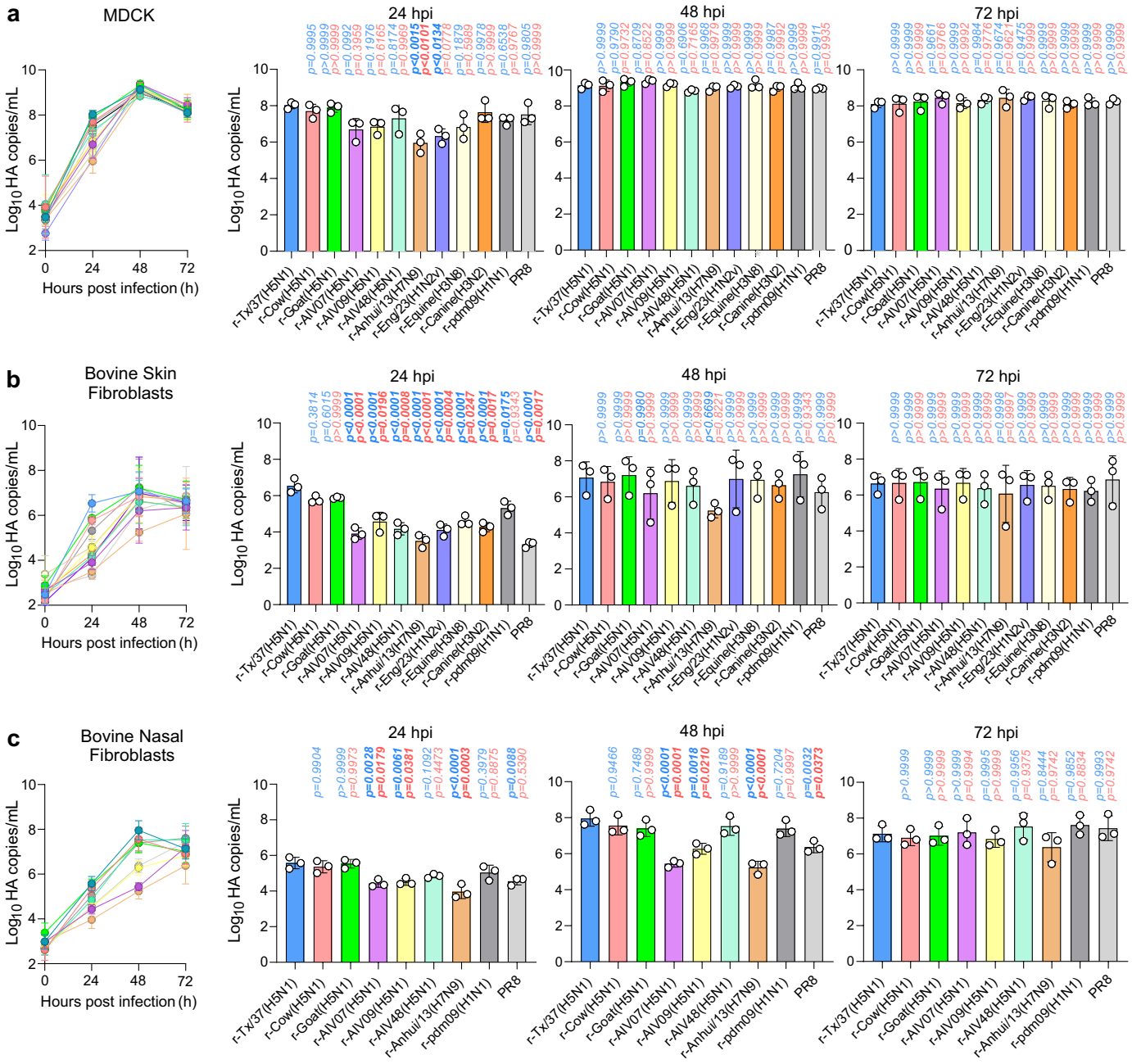
a
MDCK
24 hpi
48 hpi
72 hpi
Log10 HA copies/mL
Hours post infection (h)
r-Tx/37(H5N1)
r-Cow(H5N1)
r-Goat(H5N1)
r-AIV07(H5N1)
r-AIV09(H5N1)
r-AIV48(H5N1)
r-Anhui/13(H7N9)
r-Eng/23(H1N2v)
r-Equine(H3N8)
r-Canine(H3N2)
r-pdm09(H1N1)
PR8
b
Bovine Skin Fibroblasts
c
Bovine Nasal Fibroblasts

Fig 2

a

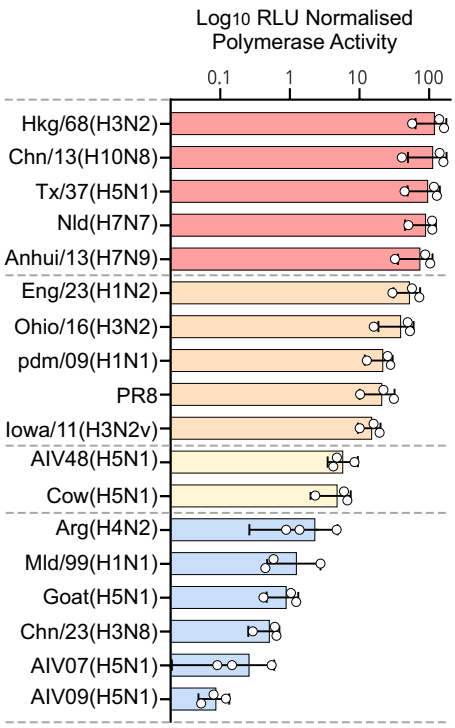

PB2 substitution									
147T	271A	339T	588T	591K	627K/V	631L	701N	702R	740N
I	A	K	I	Q	K	M	D	R	D
I	T	K	V	Q	K	M	D	K	D
I	T	K	A	Q	K	M	D	K	D
I	T	K	A	Q	K	M	D	K	D
I	T	K	A	Q	K	M	D	K	D
T	A	K	T	R	E	M	D	K	D
T	A	K	T	R	E	M	D	K	D
T	A	K	T	R	E	M	D	K	D
I	A	K	I	Q	K	M	N	K	D
T	A	K	T	R	E	M	D	K	D
I	T	K	A	Q	E	M	D	K	D
I	T	K	A	Q	E	L	D	K	D
I	T	K	A	Q	E	M	D	K	D
T	T	K	A	Q	E	M	D	K	D
I	T	K	A	Q	E	M	D	K	D
I	T	K	V	Q	E	M	D	R	D
I	T	K	A	Q	E	M	D	K	D
I	T	K	A	Q	E	M	D	K	D

b

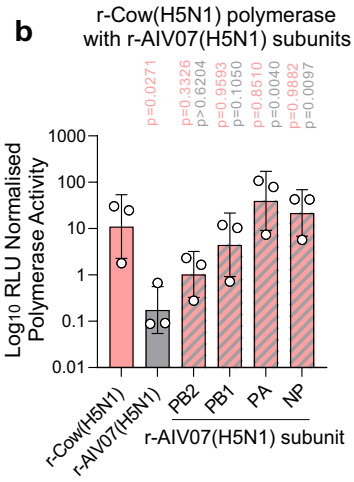

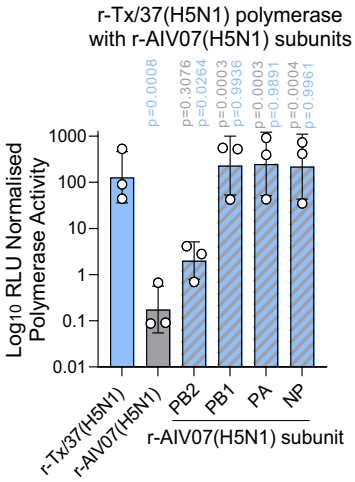

c

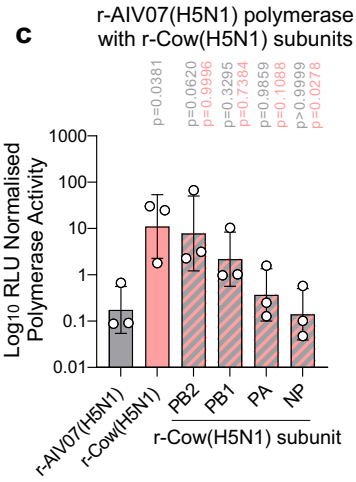

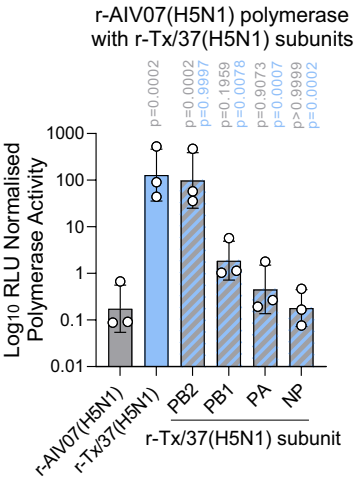

Fig 3

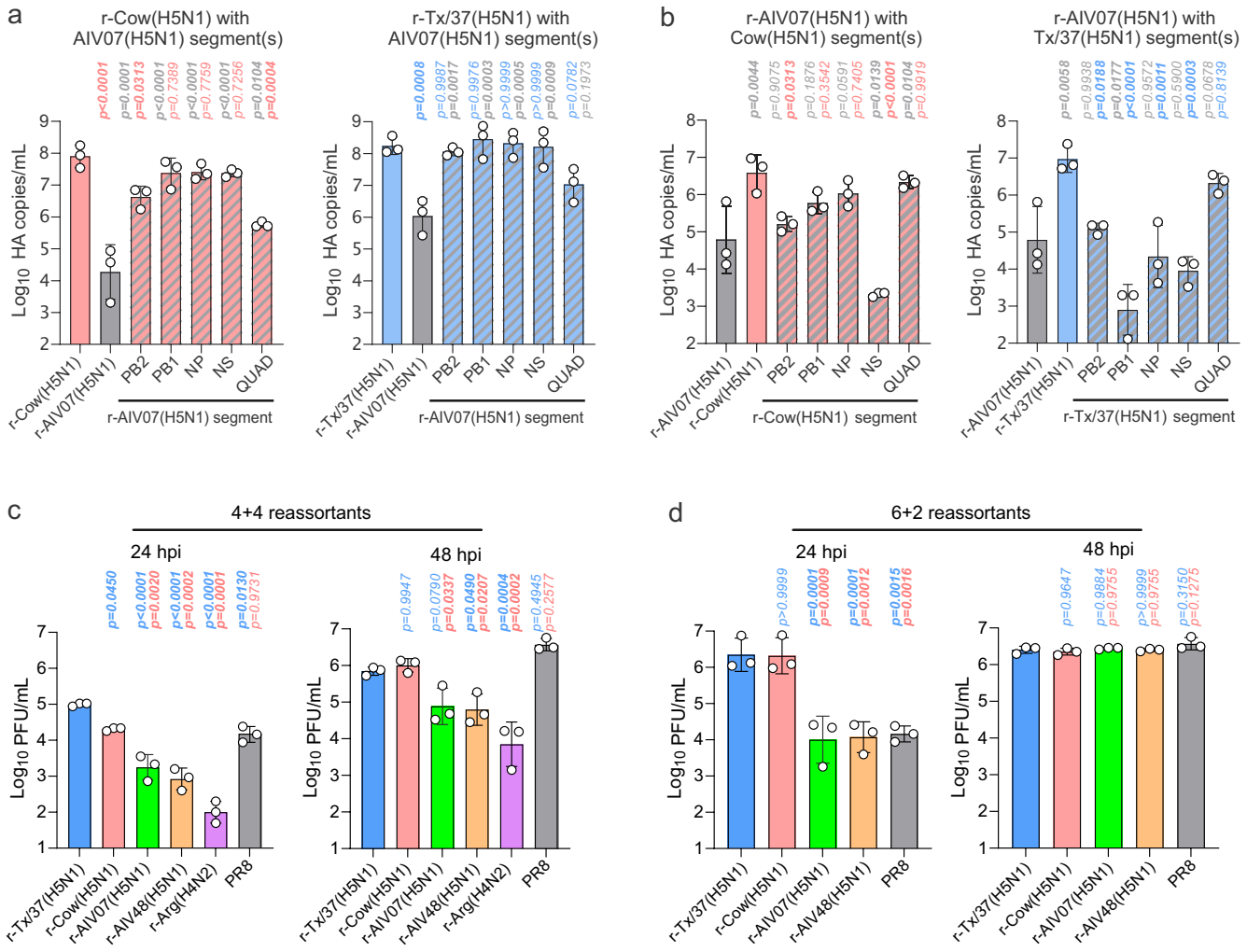
a
r-Cow(H5N1) with AIV07(H5N1) segment(s)
r-Tx/37(H5N1) with AIV07(H5N1) segment(s)
Log10 HA copies/mL
r-Cow(H5N1)
r-AIV07(H5N1)
PB2
PB1
NP
NS
QUAD
r-AIV07(H5N1) segment
r-Tx/37(H5N1)
b
r-AIV07(H5N1) with Cow(H5N1) segment(s)
r-AIV07(H5N1) with Tx/37(H5N1) segment(s)
r-Cow(H5N1) segment
r-Tx/37(H5N1) segment
c
4+4 reassortants
24 hpi
48 hpi
Log10 PFU/mL
r-Tx/37(H5N1)
r-Cow(H5N1)
r-AIV07(H5N1)
r-AIV48(H5N1)
r-Arg(H4N2)
PR8
d
6+2 reassortants

Fig 4

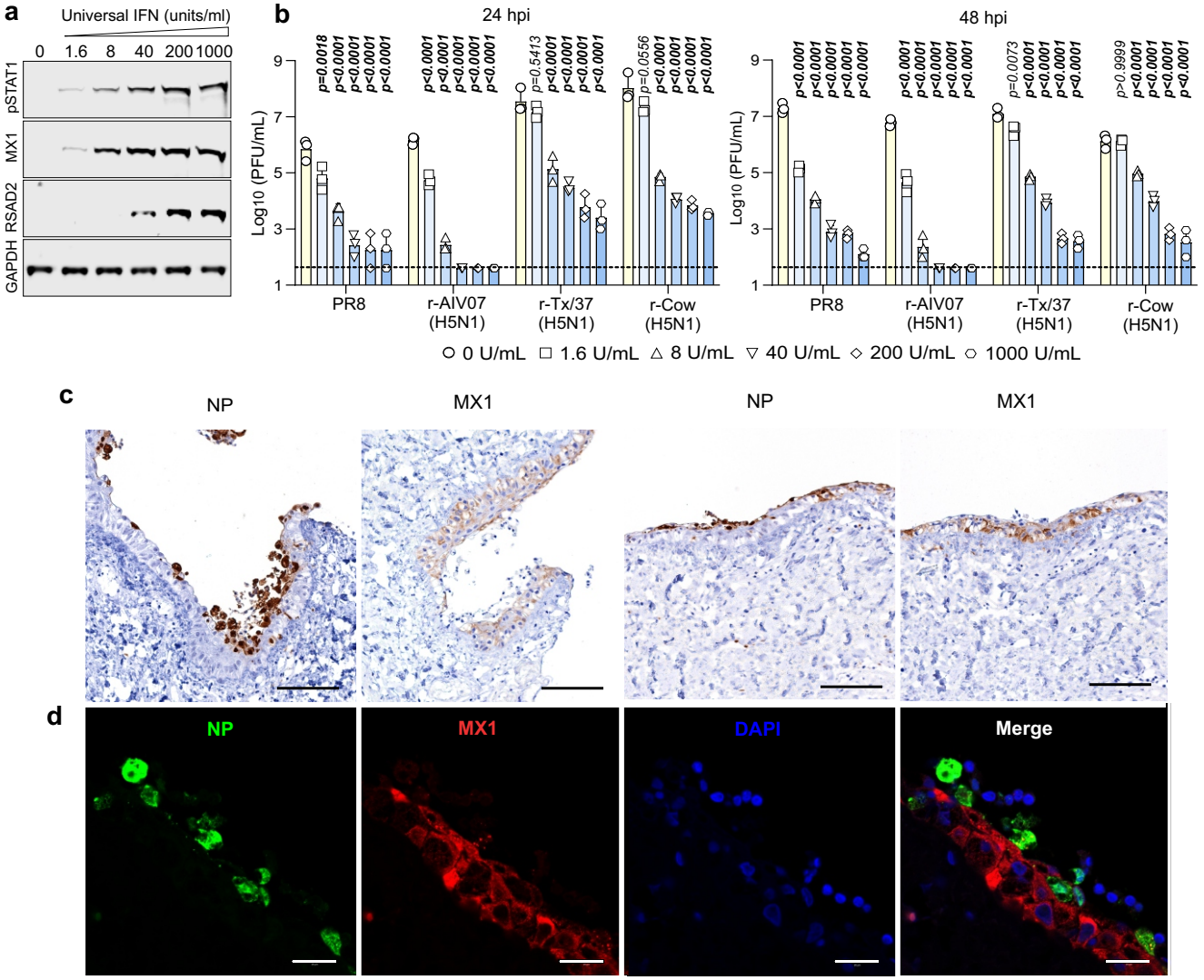
a
Universal IFN (units/ml)
0 1.6 8 40 200 1000
pSTAT1
MX1
RSAD2
GAPDH
b
24 hpi
48 hpi
Log10 (PFU/mL)
PR8
r-AIV07 (H5N1)
r-Tx/37 (H5N1)
r-Cow (H5N1)
0 U/mL
1.6 U/mL
8 U/mL
40 U/mL
200 U/mL
1000 U/mL
c
NP
MX1
d
NP
MX1
DAPI
Merge

Fig 5

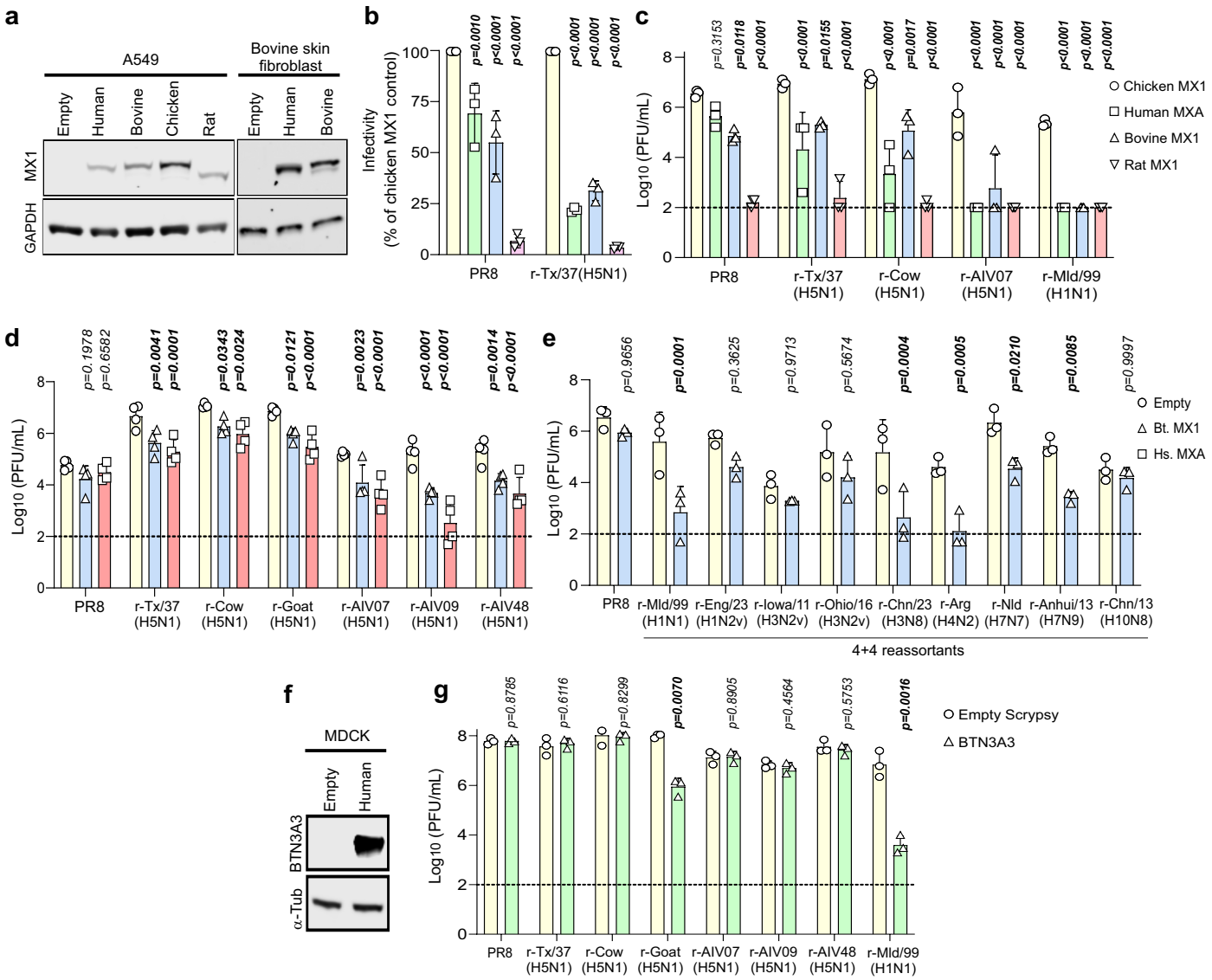
a
A549
Bovine skin fibroblast
Empty
Human
Bovine
Chicken
Rat
Empty
Human
Bovine
MX1
GAPDH
b
Infectivity (% of chicken MX1 control)
p=0.0010
p<0.0001
p<0.0001
p<0.0001
p<0.0001
p<0.0001
PR8
r-Tx/37(H5N1)
c
Log10 (PFU/mL)
p=0.3153
p=0.0118
p<0.0001
p<0.0001
p=0.0155
p<0.0001
p<0.0001
p=0.0017
p<0.0001
p<0.0001
p<0.0001
p<0.0001
p<0.0001
p<0.0001
p<0.0001
Chicken MX1
Human MXA
Bovine MX1
Rat MX1
PR8
r-Tx/37 (H5N1)
r-Cow (H5N1)
r-AIV07 (H5N1)
r-Mld/99 (H1N1)
d
Log10 (PFU/mL)
p=0.1978
p=0.6582
p=0.0041
p=0.0001
p=0.0343
p=0.0024
p=0.0121
p<0.0001
p=0.0023
p<0.0001
p<0.0001
p<0.0001
p=0.0014
p<0.0001
PR8
r-Tx/37 (H5N1)
r-Cow (H5N1)
r-Goat (H5N1)
r-AIV07 (H5N1)
r-AIV09 (H5N1)
r-AIV48 (H5N1)
e
Log10 (PFU/mL)
p=0.9656
p=0.0001
p=0.3625
p=0.9713
p=0.5674
p=0.0004
p=0.0005
p=0.0210
p=0.0085
p=0.9997
Empty
Bt. MX1
Hs. MXA
PR8
r-Mld/99 (H1N1)
r-Eng/23 (H1N2v)
r-Iowa/11 (H3N2v)
r-Ohio/16 (H3N2v)
r-Chn/23 (H3N8)
r-Arg (H4N2)
r-Nld (H7N7)
r-Anhui/13 (H7N9)
r-Chn/13 (H10N8)
4+4 reassortants
f
MDCK
Empty
Human
BTN3A3
α-Tub
g
Log10 (PFU/mL)
p=0.8785
p=0.6116
p=0.8299
p=0.0070
p=0.8905
p=0.4564
p=0.5753
p=0.0016
Empty Scrypsy
BTN3A3
PR8
r-Tx/37 (H5N1)
r-Cow (H5N1)
r-Goat (H5N1)
r-AIV07 (H5N1)
r-AIV09 (H5N1)
r-AIV48 (H5N1)
r-Mld/99 (H1N1)

Fig 6

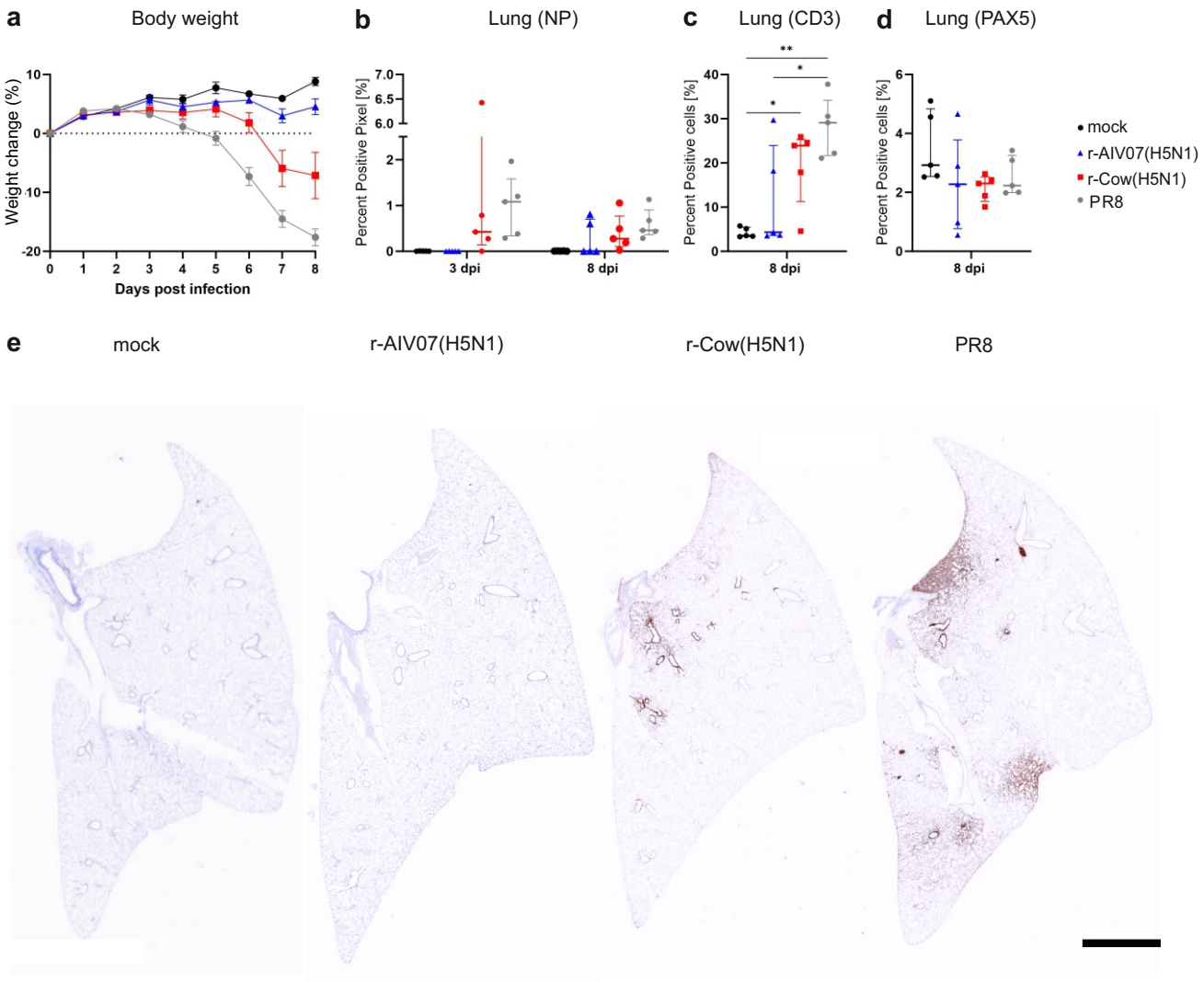
a
Body weight
Weight change (%)
Days post infection
b
Lung (NP)
Percent Positive Pixel [%]
3 dpi
8 dpi
c
Lung (CD3)
Percent Positive cells [%]
8 dpi
d
Lung (PAX5)
Percent Positive cells [%]
8 dpi
mock
r-AIV07(H5N1)
r-Cow(H5N1)
PR8
e
mock
r-AIV07(H5N1)
r-Cow(H5N1)
PR8

Fig 7

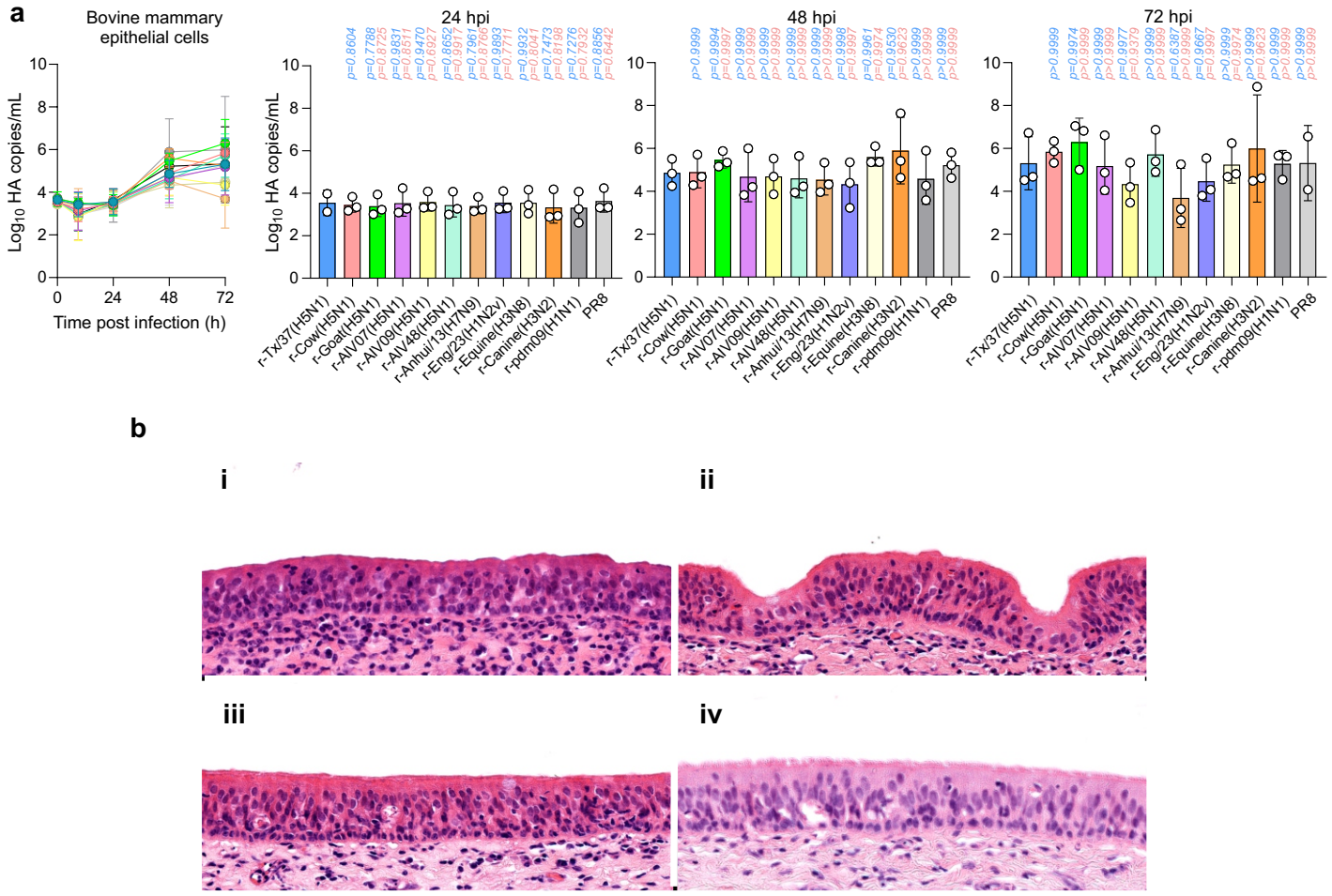
a
Bovine mammary epithelial cells
Log10 HA copies/mL
Time post infection (h)
24 hpi
48 hpi
72 hpi
r-Tx/37(H5N1)
r-Cow(H5N1)
r-Goat(H5N1)
r-AIV07(H5N1)
r-AIV09(H5N1)
r-AIV48(H5N1)
r-Anhui/13(H7N9)
r-Eng/23(H1N2v)
r-Equine(H3N8)
r-Canine(H3N2)
r-pdm09(H1N1)
PR8
b
i
ii
iii
iv

Fig S1

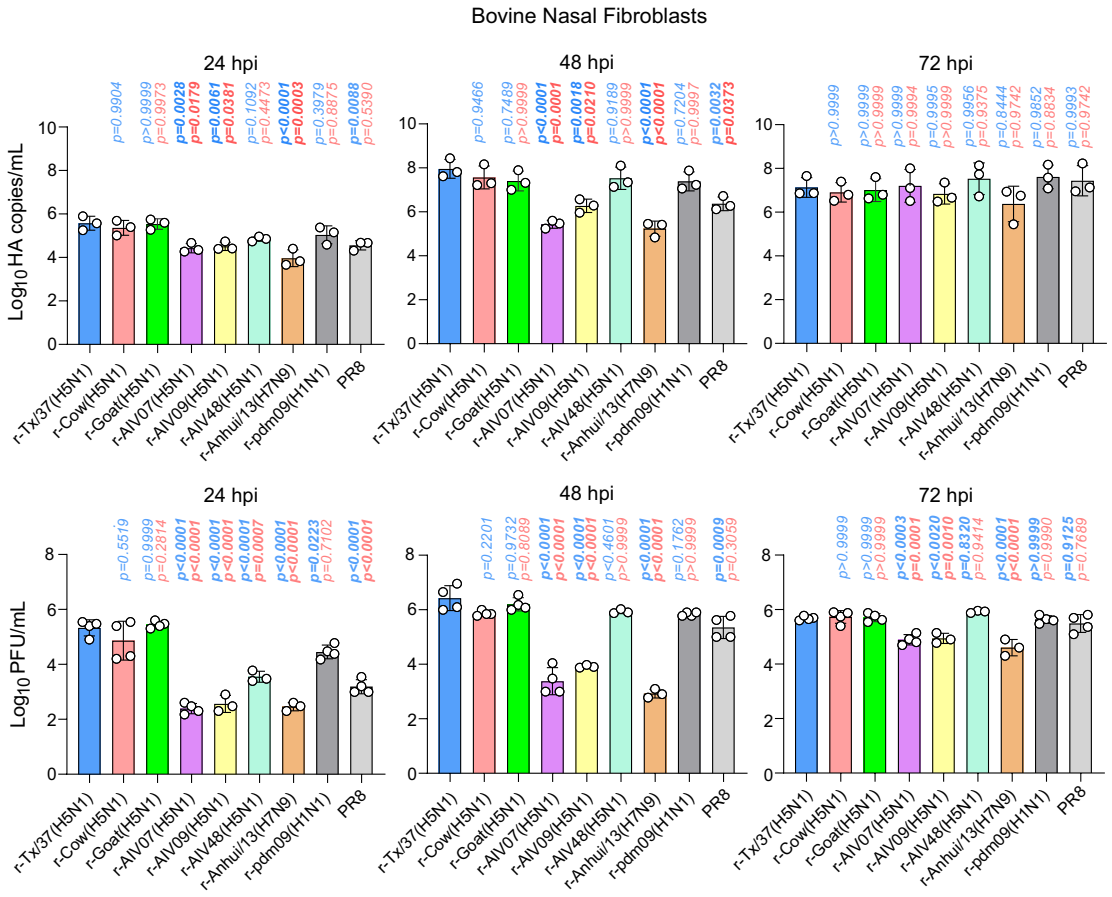
Bovine Nasal Fibroblasts
24 hpi
48 hpi
72 hpi
Log10 HA copies/mL
Log10 PFU/mL
r-Tx/37(H5N1)
r-Cow(H5N1)
r-Goat(H5N1)
r-AIV07(H5N1)
r-AIV09(H5N1)
r-AIV48(H5N1)
r-Anhui/13(H7N9)
r-pdm09(H1N1)
PR8

Fig S2